NRC immune receptor networks show diversified hierarchical genetic architecture across plant lineages

Foong-Jing Goh[1,2,3], Ching-Yi Huang[1], Lida Derevnina[4], and Chih-Hang Wu[1,2,5*]

[1]Institute of Plant and Microbial Biology, Academia Sinica, Taipei, Taiwan

[2]Molecular and Biological Agricultural Sciences Program, Taiwan International Graduate Program, National Chung-Hsing University and Academia Sinica, Taipei, Taiwan

[3]Graduate Institute of Biotechnology, National Chung-Hsing University, Taichung, Taiwan

[4]Crop Science Centre, Department of Plant Science, University of Cambridge, Cambridge, United Kingdom

[5]Biotechnology Center, National Chung-Hsing University, Taichung, Taiwan

*Correspondence: wuchh@gate.sinica.edu.tw

Short title: Diversity of NRC networks in asterids

One-sentence summary: The NRC networks show degrees of complexity across asterids, encompassing largely conserved NRC0 networks and diversified family-specific NRC networks

Abstract

Plants developed sophisticated immune systems consisting of nucleotide-binding domain and leucine-rich repeat-containing (NLR) proteins to repel invading pathogens. The NRC (NLR required for cell death) family is a group of helper NLRs that form a complex genetic network with multiple sensor NLRs to provide resistance against various pathogens of solanaceous plants. However, how the NRC network has evolved and how it functions outside of solanaceous plants is currently unknown. We conducted phylogenomic and macroevolutionary analyses comparing NLRs identified from different lineages of asterids and found that NRC networks showed significant lineage-specific expansion patterns in lamiids but not in Ericales and campanulids. Using transient expression assays in *Nicotiana benthamiana*, we show that the NRC networks in Ericales and campanulids are simple, with one or two NRC nodes, while the NRC networks of lamiids were complex, with multiple partially redundant NRC nodes. Phylogenetic analyses

grouped the NRC helper NLRs into three NRC0 subclades that are conserved, and several family-specific NRC subclades of lamiids that show signatures of diversifying selection. Functional analyses of NRCs and NRC-dependent sensor NLRs from different species revealed that members of the NRC0 subclades are partially interchangeable, with several functioning with NRC0-dependent sensor NLRs across asterids. In contrast, family-specific NRC members in lamiids display a lack of interchangeability, with only a few showing compatibility with sensor NLRs across different plant families. Our findings highlight the distinctive evolutionary patterns of the NRC networks in asterids and provide potential insights into transferring disease resistance across plant lineages.

Keywords: plant immunity, disease resistance genes, nucleotide-binding domain and leucine-rich repeat-containing protein (NLR), NLR-required for cell death (NRC), immune receptor network, evolution, asterids

Introduction

Plants have evolved intricate immune systems to protect themselves from pathogen invasion. Intracellular nucleotide-binding domain and leucine-rich repeat (NLR) immune receptors play major roles in plant immunity by detecting effector proteins delivered from pathogens (Dodds and Rathjen, 2010; Jones et al., 2016; Ngou et al., 2022). NLR activation often results in a form of programmed cell death known as the hypersensitive response, leading to the restriction of pathogen growth. NLRs exhibit a conserved tripartite structure comprised of an N-terminal domain involved in cell death initiation, a central nucleotide-binding domain (NBD) involved in activation, and a C-terminal leucine-rich repeat (LRR) domain involved in ligand binding and NLR self-regulation (Duxbury et al., 2021). NLRs are classified based on their N-terminal domains into TNLs that contain Toll/interleukin-1 receptor/R protein (TIR) domains, RNLs that contain Resistance to Powdery mildew 8 (RPW8)-like coiled-coil (CC) domains, and CNLs that contain G10-type or Rx-type coiled-coil domains (Shao et al., 2016; Duxbury et al., 2021; Lee et al., 2021; Kourelis et al., 2021).

Molecular and genetic studies have categorised NLRs into three groups based on their mode of action: singletons, pairs, and networks (Contreras et al., 2023b). Singleton NLRs can directly or indirectly detect pathogen effectors and initiate downstream immune responses without the assistance of additional NLRs (Kourelis and Van Der Hoorn, 2018; Contreras et al., 2023b). The CNLs ZAR1 (HopZ-Activated Resistance 1) from *Arabidopsis thaliana* and Sr35 from wheat are two well-studied examples of singleton NLRs (Wang et al., 2015, 2019; Förderer et al., 2022). ZAR1 indirectly recognizes effectors via its RLCK (Receptor-like cytoplasmic kinase) partners and form pentameric membrane-associated resistosome complexes that function as calcium-

permeable channels to activate immune responses (Wang et al., 2015, 2019; Bi et al., 2021). Sr35 directly binds the stem rust effector AvrS35 through its LRR domain, forming a pentameric resistosome complex similar to ZAR1 (Förderer et al., 2022). NLRs can also function in pairs, in which a sensor NLR, specialised to recognise pathogen effectors, is coupled with a helper NLR that is involved in immune signalling. Paired NLRs often physically interact and exist as linked gene pairs or clusters on the chromosomes, suggesting that they are co-regulated and may have co-evolved exclusively with each other throughout their evolutionary trajectory (Xi et al., 2022). Classical examples of paired NLRs include RRS1/RPS4 of *A. thaliana*, and RGA4/RGA5 and Pik-1/Pik-2 of rice (Ashikawa et al., 2008; Narusaka et al., 2009; Césari et al., 2014; Sohn et al., 2014; Xi et al., 2022). In these pairs, the sensor NLRs often contain integrated domains (ID) that play critical roles in sensing pathogen effectors; for example, the WRKY domain in RRS1 and HMA (Heavy-Metal-Associated) domain in RGA5 and Pik-1 (Cesari et al., 2013; Maqbool et al., 2015; Sarris et al., 2015; Marchal et al., 2022).

NLRs can also function in networks, in which multiple sensor NLRs that detect different pathogen effectors signal through a set of helper NLRs to mediate immunity (Wu et al., 2017, 2018). NRG1 (N-Required Gene 1) and ADR1 (Activated Disease Resistance 1), two RNL-type helper NLRs, are required by multiple sensor NLRs for immune signalling (Castel et al., 2019; Saile et al., 2020). In Arabidopsis, the TNLs RPS4/RRS1, RPP2, and RPS6, preferentially signal through NRG1, whereas the CNLs RPS2 and RPP4 preferentially signal through ADR1, supporting the idea that the two groups of helper NLRs show complex genetic redundancy (Saile et al., 2020). Similar to NRG1 and ADR1, NRCs (NLR-required for cell death) are required by multiple Solanaceae sensor NLRs. Within the NRC network, the NRC-dependent sensor NLRs detect different pathogen effectors and require partially redundant helper NRCs for immune response. For example, sensor NLRs Rpi-blb2, Mi-1.2, and R1 transmit signals via NRC4 to trigger cell death. The sensor NLR Prf and Rpi-amr1 operates with either NRC2 or NRC3, while Sw5b, R8, Rx, Bs2, and Rpi-amr3 can signal redundantly through NRC2, NRC3, or NRC4 (Wu et al., 2017, 2016; Chen et al., 2021; Witek et al., 2021; Wu and Kamoun, 2021; Lin et al., 2022).

Phylogenetically, NRCs and NRC-dependent sensor NLRs form the NRC superclade, which is a subgroup of Rx-type CNLs (Wu et al., 2017; Kourelis et al., 2022). The NRC superclade is present across the asterids and in some Caryophyllales, but is not present in monocots or rosids. This suggests that the ancestral sequences of the NRC superclade arose more than 100 million years ago, predating the diversification of Caryophyllales and asterids (Wu et al., 2017). A recent report defined NRC0, an NRC helper NLR, as the only conserved family member found in various asterids. NRC0 often exists in a gene cluster with NRC0-dependent sensor NLRs, strengthening the hypothesis that the NRC superclade originated from an ancient helper-sensor NLR gene cluster (Wu and Kamoun, 2021). Another intriguing evolutionary aspect of the NRC superclade is the presence of noncanonical extended N-terminal domains (exNT), which exist before the CC domain in some clades of sensor NLRs (Seong et al., 2020; Adachi et al., 2023a). Although the detailed evolutionary history of the sensor NLRs is not clear, the exNT were also found in sugar beet,

106 suggesting that the exNT of NRC-dependent sensor NLRs emerged between the common ancestor
107 of asterids and Amaranthaceae (Caryophyllales) (Seong et al., 2020).

108 Upon sensor NLR activation, NRCs form higher-molecular-weight complexes that localize to the
109 plasma membrane and likely act as calcium-permeable channels similar to ZAR1 (Ahn et al., 2023;
110 Contreras et al., 2023a). The first alpha helixes of most NRCs possess a conserved α1 helix domain
111 known as the MADA motif that plays a major role in executing cell death (Adachi et al., 2019).
112 The MADA motif is conserved in ZAR1 and many other singleton NLRs but is absent in the NRC-
113 dependent sensor NLRs, suggesting that degeneration of the MADA motif may be an evolutionary
114 feature associated with the functional diversification of the NRC superclade members (Adachi et
115 al., 2019). Interestingly, members of the NRC family have also evolved functions beyond
116 triggering cell death induced by sensor NLRs. The cell surface receptor Cf-4 induces NRC3-
117 dependent hypersensitive responses upon detection of the plant pathogen effector AVR4,
118 indicating that the NRC superclade not only functions in intracellular receptor defence but also
119 contributes to cell surface receptor-mediated defences (Kourelis et al., 2022). Furthermore, NRCx,
120 an unusual NRC family member lacking a functional MADA motif, modulates NRC2/NRC3-
121 mediated cell death in *Nicotiana benthamiana* plants. NRCx functions as a negative regulator of
122 cell death execution, thus, playing a key role in maintaining homeostasis within the NRC network
123 (Adachi et al., 2023a).

124 NLRs represent one of the most diverse protein families in angiosperms, with many species
125 encoding large and diverse repertoires of NLR genes in the genome (Barragan and Weigel, 2021).
126 As they play key roles in the survival of a plant species under emerging pathogen pressures, *NLR*
127 genes are known to show distinguished signs of rapid evolution, even within a single species
128 (Kuang et al., 2004; Jacob et al., 2013; Van De Weyer et al., 2019). Given that NLRs exhibit a
129 high turnover rate, the birth-and-death model has been proposed to describe the evolutionary
130 process of *NLR* genes (Michelmore and Meyers, 1998). In this model, the emergence of new NLRs
131 occurs through repetitive cycles of gene duplication. Some genes are maintained in the genome
132 and develop novel capabilities to detect pathogens, while others are either lost or nonfunctionalized
133 due to the accumulation of deleterious mutations (Michelmore and Meyers, 1998; Barragan and
134 Weigel, 2021). These dynamic evolutionary patterns allow the plant immune system to effectively
135 adapt to the rapidly evolving effector repertoires of pathogenic microbes. Indeed, some NLRs have
136 been lost in certain plant lineages but highly expanded in other plant lineages (Shao et al., 2016;
137 Martin et al., 2023). TNLs and RNLs (particularly NRG1), along with their associated signalling
138 partner SAG101, have been lost in monocots, some dicots, and some Magnoliids (Tarr and
139 Alexander, 2009; Collier et al., 2011; Shao et al., 2016; Liu et al., 2021; Wu et al., 2021). However,
140 these two groups of NLRs are more highly expanded and diversified in Gymnosperms and Rosids
141 (Terefe-Ayana et al., 2012; Andolfo et al., 2019; Van De Weyer et al., 2019). CNLs are in general
142 more abundant in the genomes of most angiosperms, whereas TNLs have been lost frequently in
143 dicots (Liu et al., 2021). Studies of wild tomato and Arabidopsis demonstrated a wide range of
144 NLR polymorphisms within single-species populations, suggesting a correlation between plant

145 adaptation to pathogens and NLR diversity (Stam et al., 2019; Van De Weyer et al., 2019). These
146 NLR polymorphisms may contribute to species-specific signalling pathways in NLR-mediated
147 resistance. For example, CaRpi-blb2, a pepper homolog of wild tomato Rpi-blb2, initiates cell
148 death via NRC8 and NRC9 which were identified only in pepper but not other solanaceous species,
149 highlighting the contribution of lineage-specific NLR clades that emerged recently in resistance
150 against pathogens (Oh et al., 2023).

151 The availability and improvement of genome databases have enabled the analyses of NLR genes
152 from many model and non-model species, leading to a more comprehensive understanding of NLR
153 evolution and diversity (International Wheat Genome Sequencing Consortium et al., 2018; Van
154 De Weyer et al., 2019; Barragan and Weigel, 2021; Kourelis et al., 2021; Ence et al., 2022). Plant
155 NLRs likely originated from the common ancestor of green algae before rapidly diversifying and
156 evolving in land plants (Gao et al., 2018; Ortiz and Dodds, 2018; Shao et al., 2019). The discovery
157 of the MAEPL motif and the MADA motif, which are both crucial in executing cell death, provides
158 evidence of the shared function of the CC domain between non-flowering and flowering plants,
159 strengthening the concept of the origin of NLR from common green algae (Adachi et al., 2019;
160 Chia et al., 2022). While a high number of NLR genes could offer potential survival advantages,
161 several factors have been proposed to influence the number of NLR genes in a particular plant
162 species. Adaptations to aquatic, parasitic, and carnivorous lifestyles correlated to low NLR
163 numbers among closely related species (Baggs et al., 2020; Liu et al., 2021). For example, the
164 aquatic plant *Lemna minor* (duckweed) has only 11 NLR genes, and the carnivorous aquatic plant
165 *Utricularia gibba* has completely lost all NLR genes (Baggs et al., 2020; Liu et al., 2021). To date,
166 close to 500 NLRs from 31 genera belonging to 11 orders of flowering plants have been
167 experimentally validated (Kourelis et al., 2022). These NLRs emerged in different plant species
168 and likely diversified to function against various pathogens. The diversity of NLRs found in plants
169 may reflect the outcome of their long-standing coevolutionary arms race with pathogens (Upson
170 et al., 2018).

171 Asterids constitute highly diverse groups of angiosperms and encompass numerous economically
172 important crops. The NRC superclade exists in several asterids species, suggesting that NRC
173 networks may play roles in disease resistance in these plants (Wu et al., 2017; Sakai et al., 2023).
174 Understanding the diversity of NRC networks across asterids may provide useful information on
175 lineage- or species-specific sensor-helper NLR connections, which could be useful for disease
176 resistance breeding and help facilitate interspecies resistance gene transfer. However, our
177 knowledge of the evolutionary history and diversity of NRC networks beyond Solanaceae is
178 limited. To address this, we performed macroevolutionary analyses of NRC networks across
179 asterids and experimentally validated the sensor-helper dependency using heterologous expression
180 in *N. benthamiana*. We found that the NRC superclade displays distinct duplication and expansion
181 patterns in the three asterids lineages (Ericales, campanulids, and lamiids). Combined with the
182 results from transient expression assays in *N. benthamiana*, we revealed that the NRC networks in
183 Ericales, campanulids, and lamiids show different complexity and hierarchical structures. The

184 NRC helper NLR family can be further grouped into three NRC0 subclades that are conserved,
185 and several family-specific NRC subclades of lamiids that show signatures of diversifying
186 selection. Further inter-species comparisons revealed that members of the NRC0 subclades were
187 partially interchangeable, as many of them can function with NRC0-dependent sensor NLRs from
188 different lineages. In contrast, members of the family-specific NRC subclades of lamiids lack
189 interchangeability, with only some of the NRCs showing compatibility with sensor NLRs across
190 plant families. Our study sheds light on the unique evolutionary patterns of the NRC networks
191 within the asterids and offers valuable insights into the potential transfer of disease resistance
192 mechanisms across different plants.

193

194 **Results**

195 **The NRC superclade is expanded differentially in distinct plant lineages**

196 To understand the evolutionary diversity of the NRC network in plants, we performed comparative
197 phylogenomic analyses of 46 angiosperms, including basal angiosperms, monocots, rosids,
198 Caryophyllales, and asterids (comprising Ericales, campanulids and lamiids) (Supplemental Data
199 Set 1). We used MAST - MEME Suite and 20 previously defined motifs to predict potential NLR
200 encoding sequences from the genome of all these angiosperms (Jupe et al., 2012; Steuernagel et
201 al., 2015). After generating the NLR phylogenetic trees of each species using the conserved NB-
202 ARC domain, we grouped these NLRs into four categories including TNL, RNL, CC_{G10}-NLR, and
203 the CC_{Rx}-NLR. To identify the NRC superclades in these species, we performed additional
204 phylogenetic analyses of the CC_{Rx}-NLR using the solanaceous NLRs (NRC, NRC-dependent and
205 NRC-independent NLRs) as references. These second phylogenetic trees classified the CC_{Rx}-NLR
206 into the NRC superclade and non-NRC superclade CNLs. Consistent with the previous finding,
207 the NRC superclade was found only in species of some Caryophyllales and most asterids
208 (Supplemental Data Set 2) (Wu et al., 2017).

209 Next, we calculated the percentage of NRC superclade members relative to the total number of
210 NLRs in these genomes (Fig. 1A). Interestingly, the percentages of NRC superclade members
211 relative to the total number of NLRs show striking variations across different plant lineages. In
212 Caryophyllales, two out of the seven species we analysed contained the NRC superclade (Fig. 1A).
213 *Beta vulgaris* and *Dianthus caryophyllus* have approximately 4% and 15% of their total NLRs
214 belonging to the NRC superclade, respectively. In Ericales, all three species we analysed contain
215 members of the NRC superclade (Fig. 1A). The percentages of NRC superclade members out of
216 total NLR in *Actinidia chinensis*, *Camelia sinensis* and *Synsepalum dulcificum* are 7%, 3% and
217 1%, respectively. In campanulids, the percentage of NLRs belonging to the NRC superclade is
218 variable, with an average of 8% out of total NLRs (Fig. 1A). Among the campanulids analysed,
219 *Panax ginseng* has the lowest percentage of NRC superclade members, with 3% (4 out of 131) of
220 its NLRs belonging to the NRC superclade; *Stevia rebaudiana* has the highest percentage, with

221 14% (44 out of 298) of its NLRs belonging to the NRC superclade. In lamiids, the proportions of
222 NRC superclade members among total NLRs are highly variable (Fig. 1A). Overall, the number
223 of NRC superclade members in lamiids is higher than that of Caryophyllales, Ericales, and
224 campanulids. In most lamiids species, over 40% of the total NLRs belong to the NRC superclade.
225 In tomato, where the NRC superclade and NRC network were originally described (Wu et al.,
226 2017), 46.7% of total NLRs belong to the NRC superclade. In contrast, over 75% of total NLRs
227 from the three related *Ipomoea* species (*I. batatas*, *Ipomoea trifida* and *Ipomoea triloba*) belong
228 to the NRC superclade (Fig. 1A). Remarkably, *Striga asiatica*, a parasitic plant, has the highest
229 percentage (89%) of NRC superclade members among all analysed plant species, while *Cuscuta*
230 *australis*, another parasitic plant, has the lowest percentage (14%) of NRC superclade members
231 among lamiids, with only one out of seven NLRs belonging to the superclade. *Eucommia ulmoides*,
232 the rubber tree, was the only lamiids species where the NRC superclade was not found (Fig. 1A).
233 These results suggest that the NRC superclade shows very different evolutionary trajectories
234 among plant lineages.

235 To understand the degree to which the expansion of the NRC superclade and other NLRs correlates
236 with genome expansion, we compared the size of the genome or the number of protein-coding
237 genes with the number of NLRs or the size of the NRC superclade of each species. The data
238 revealed that there was no correlation between genome size with the amounts of NLRs or the size
239 of the NRC superclade (Supplemental Fig. S1A and S1B), but there was a weak correlation
240 between NLRs and the numbers of total protein-coding genes (R=0.36, p=0.052) (Supplemental
241 Fig. S1C). Additionally, the size of the NRC superclade was very weakly correlated with total
242 protein-coding genes (R=0.28, p=0.13) (Fig. 1B), suggesting that the overall evolutionary pattern
243 of total NLRs is not well aligned with that of the NRC superclade in these species. To further
244 compare the features of the NRC superclade and NLR expansion in different plant lineages, we
245 assessed the number of total NLR/total protein-coding genes and the size of the NRC
246 superclade/total protein-coding genes. The lamiids had higher ratios of total NRCs to total protein-
247 coding genes compared to other plant lineages (Supplemental Fig. S1D). Based on these analyses,
248 we concluded that the expansion of the NRC superclade is a unique characteristic of lamiids.

249 The NRC superclade encompasses two types of NLRs, namely the NRC-dependent sensor NLRs
250 (NRC-S) and the NRC helper NLRs (NRC-H). Since the NRC superclade originated from a linked
251 NLR pair or cluster, we expect the ancestral sensor-helper ratio of the NRC superclade to be around
252 1:1 or 2:1. To gain further insights into whether the sensor and helper NLRs within the NRC
253 superclade have expanded differentially during evolution, we calculated the NRC sensor-helper
254 ratio for all NRC superclade containing plant species (Fig. 1C). Most of the species have NRC
255 sensor-helper ratios greater than 2:1, suggesting that the NRC-S experience more frequent
256 duplication events in comparison to NRC-H. In Ericales and campanulids, where the NRC
257 superclade constitutes only a small portion of total NLRs, the NRC sensor-helper ratio varied. In
258 Ericales, the NRC sensor-helper ratio ranged from 1:1 to 4:1, while in campanulids this ratio
259 ranged from 3:1 to 14:1. In lamiids, where the NRC superclade is extensively expanded, most

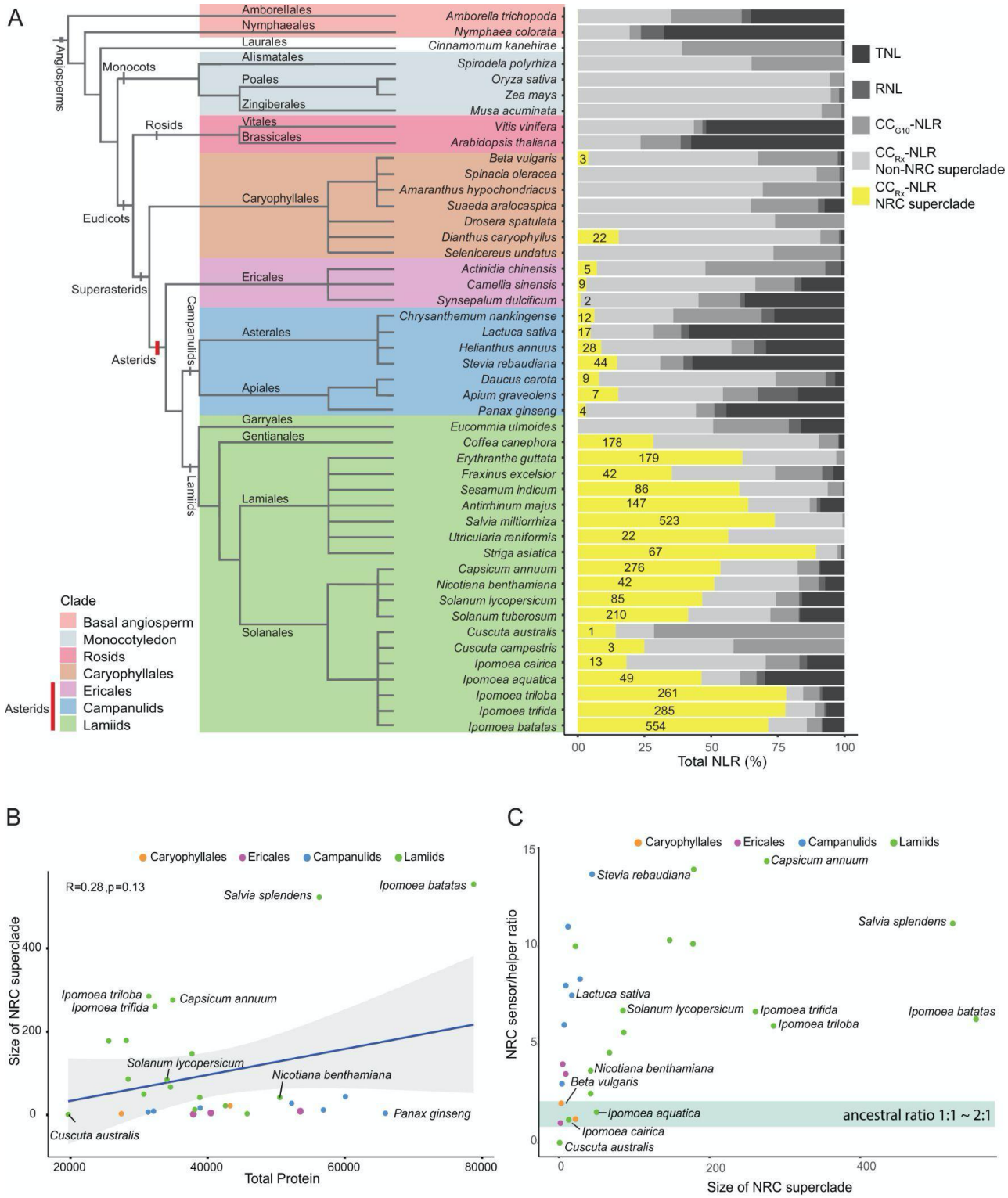

Figure 1. The expansion of the NRC superclade is a unique feature of lamiids. **A)** (Left) Phylogenetic tree of angiosperm species, modified from The Angiosperm Phylogeny Group (2016). (Right) Percentage and number of different types of NLRs identified from each species. Numbers in the stacked bar chart indicate the sizes of NRC superclade members in the plant species. **B)** Correlation between the size of the NRC superclade and the number of total protein-coding genes. **C)** Comparisons of the NRC sensor-helper ratio and the size of the NRC superclade. The highlighted area indicates the ancestral ratio of the NRC sensor and helper, which is close to 1:1 to 2:1. Plant species from different lineages are labelled with different colours.

261 species displayed sensor-helper ratios higher than the ancestral ratio (Fig. 1C). Together, these
262 findings indicate that sensor NLRs are more prone to duplication during evolution compared to
263 helper NLRs, supporting the notion that sensor NLRs require diversification to recognise various
264 pathogens, while helper NLRs are involved in mediating a conserved cell death pathway.

265 **The NRC network in Ericales is simple**

266 To characterise the NRC superclade in Ericales, we performed phylogenetic analysis on NLRs
267 identified from *A. chinensis*, *C. sinensis*, and *S. dulcificum* using tomato NRC superclade members
268 as a reference (Fig. 2, A and B). The Ericales NRC superclade can be divided into one NRC-H
269 clade and one NRC-S clade. To understand the phylogenetic relationship of the Ericales NRCs
270 with the NRC0 subclade described by Sakai et al. (2023), we performed phylogenetic analyses
271 encompassing all the predicted NRC-H from asterids. We found the Ericales NRC-H clustered
272 together with the NRC0 subclade, but formed its lineage-specific group (Supplemental Fig S2A).
273 Therefore, to differentiate this group of NRCs from the NRC0 subclade, we named the members
274 of this subclade NRC0-Ericales-specific (NRC0-Eri). In several plant species, NRC0 orthologs are
275 physically clustered with the NRC0-dependent sensor NLRs on the chromosome (Sakai et al.,
276 2023). We found a putative NRC-S linked to one of the NRC0-Eri in *C. sinensis* (CsNRC0b-Eri)
277 (Supplemental Fig. S2B and C), but no sensor-helper linkage was found in *A. chinensis* or *S.*
278 *dulcificum*.

279 To validate that the members of NRC0-Eri function as helper NLRs for the putative sensor NLRs,
280 we cloned NRC0 from *A. chinensis* (AcNRC0-Eri) and *C. sinensis* (CsNRC0a-Eri) and performed
281 transient expression assays in *N. benthamiana* together with putative sensor NLRs from the same
282 species. As CsNRC0b-Eri is truncated and expression of AcNRC0-Eri alone induced cell death in
283 wild type and *nrc2/3/4*_KO *N. benthamiana,* we focused on CsNRC0a-Eri for validation of the
284 Ericales NRC network (Supplemental Fig. S2D). Out of the 7 putative NRC-dependent sensor
285 NLRs from the genome of *C. sinensis*, two contained full-length NLR sequence signatures, and
286 the remaining five were truncated. We cloned the two full-length *C. sinensis* NLRs (Cs0021741
287 and Cs0024074) and introduced a D to V mutation into their MHD motifs to generate constitutively
288 active variants ($Cs0021741^{DV}$ and $Cs0024074^{DV}$). Co-expression of $Cs0024074^{DV}$, but not
289 $Cs0021741^{DV}$, with CsNRC0a-Eri induced cell death in *N. benthamiana.* Cell death was not
290 observed when either $Cs0024074^{DV}$ or CsNRC0a-Eri were expressed alone, suggesting that
291 CsNRC0a-Eri, indeed, functions as a helper NLR (Fig. 2C). Overall, our data suggests that the
292 NRC network of Ericales is simple, with few sensor NLRs signalling through one or two NRC0
293 homologs (Fig. 2D).

294

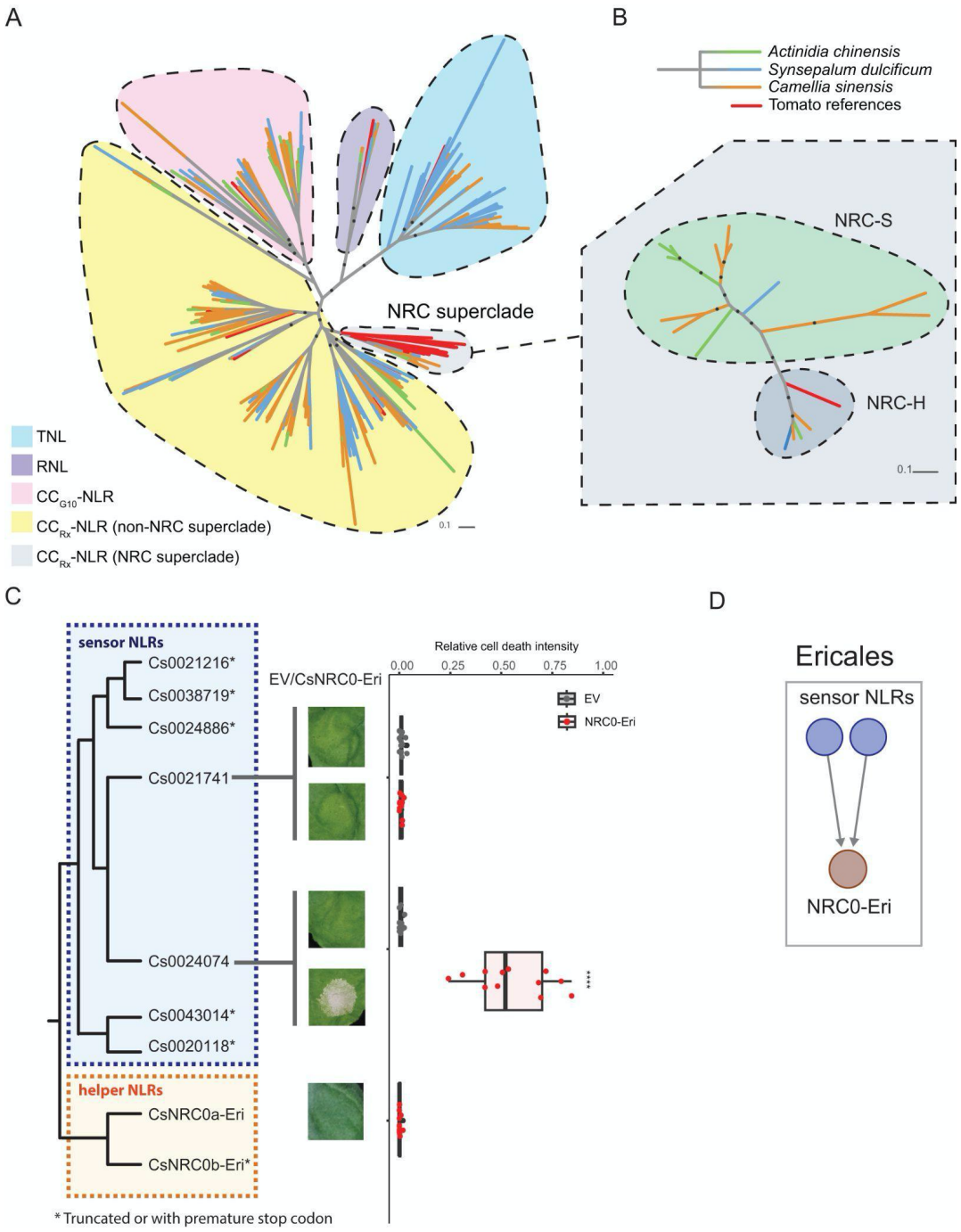

Figure 2. Ericales encode a simple NRC network, with sensor NLRs signalling through NRC0-Eri to initiate cell death. **A)** Phylogenetic analysis of total NLRs from 3 Ericales species, including *A. chinensis*, *S. dulcificum*, and *C. sinensis.* NLRs from different species are indicated with lines of different colours. NLR sequences from the tomato NRC superclade were used as references. **B)** Phylogenetic analysis of the NRC superclade from the 3 Ericales species with tomato NRC0 as reference sequences. For both phylogenetic trees, major branches with bootstrap values higher than 70 are indicated with black dots. **C)** Cell death assay was performed by co-expression of the putative NRC0-Eri-dependent sensor NLR from tea (*C. sinensis*) and tea CsNRC0a-Eri. All sensor NLRs carried the MHD motif (D to V) mutation. The intensity of cell death was analysed at 5 dpi. The dot plot represents the relative cell death intensity based on autofluorescence imaging using UVP ChemStudio PLUS. Statistical differences were examined by paired Student's t-test (**** = $p < 0.0001$; * = $p < 0.05$). **D)** Putative NRC network structure in Ericales where few sensor NLRs signal through Ericales NRC0 (NRC0-Eri) to induce cell death.

295

296 **NRCs duplicated in some campanulids, forming an NLR network with partially redundant**
297 **nodes**

298 To characterise the NRC superclade in campanulids, we performed phylogenetic analyses of NLRs
299 identified from seven species, including *Chrysanthemum nankingense, Lactuca sativa, Helianthus*
300 *annuus, S. rebaudiana, Daucus carota, Apium graveolens*, and *P. ginseng*, across two major orders
301 (Asterales and Apiales) (Supplemental Fig. S3A). In line with our previous findings, the
302 campanulids NLRs were classified into several highly supported clades consisting of TNLs, RNLs,
303 CC_{G10}-NLRs and CC_{Rx}-NLRs, which include the NRC superclade (Fig. 3A and Supplemental Fig.
304 S3A). Phylogenetic analysis revealed that the campanulids NRC superclade is divided into
305 multiple clades, including one NRC-H clade and several putative NRC-S clades (Fig. 3B). The
306 NRC-H clade can be further divided into the NRC0 subclade, which contains sequences from both
307 Asterales, Apiales and the reference tomato NRC0, as well as another subclade which contains
308 sequences only from the Asterales (Fig. 3B). Based on the phylogenetic tree of NRC-H from
309 asterids, this subclade clusters together with NRC0-Eri and the NRC0 subclade defined by Sakai
310 et al. (2023) (Supplemental Fig. S2A). Therefore, we named this group the NRC0-Asterales-
311 specific (NRC0-Ast) subclade.

312 To determine the genetic structure of the campanulids NRC network, we selected *D. carota* (carrot)
313 from Apiales and *L. sativa* (lettuce) from Asterales as representative species. The carrot NRC
314 superclade is comprised of DcNRC0 and eight sensor NLRs falling into two subgroups (Fig. 3B
315 and Supplemental Fig. S3, B and C). Out of the eight sensor NLRs, two of them (Dc23557 and
316 Dc23650) are located in a gene cluster together with DcNRC0 (Supplemental Fig. S3D). We
317 cloned four putative sensor NLRs, including Dc23557 and Dc23650, and introduced a D to V
318 mutation into their MHD motifs and then co-infiltrated them independently with DcNRC0. Of
319 these, only $Dc23557^{DV}$ and $Dc23650^{DV}$ induced cell death in the presence of DcNRC0
320 (Supplemental Fig. S3E). The lettuce NRC superclade is composed of LsNRC0, LsNRC0-Ast, and
321 15 sensor NLRs. These sensor NLRs are clustered into two sub-groups (Supplemental Fig. S4A).
322 LsNRC0 is located in proximity to some of the sensor NLRs whereas LsNRC0-Ast is located on
323 a different chromosome (Supplemental Fig. S3, B and C). Similar to the previous experiment, we
324 introduced autoactive mutations (D to V) into the MHD motif of the sensor NLRs, and then
325 performed cell death assays by co-agroinfiltration with either LsNRC0 or LsNRC0-Ast on *N.*
326 *benthamiana* leaves. Two putative sensor NLRs within the same sensor NLR sub-group
327 ($Ls123301^{DV}$ and $Ls124100^{DV}$) induced cell death when co-expressed with LsNRC0 but not
328 LsNRC0-Ast. Three members of the other sensor NLR sub-group ($Ls35940^{DV}$, $Ls28800^{DV}$, and
329 $Ls36021^{DV}$) induced cell death when co-expressed with LsNRC0-Ast but not LsNRC0 (Fig. 3C).
330 Interestingly, one of these putative sensor NLRs ($Ls124601^{DV}$) induced cell death when co-
331 expressed with either LsNRC0 or LsNRC0-Ast (Fig. 3C). These results indicate that the sensor

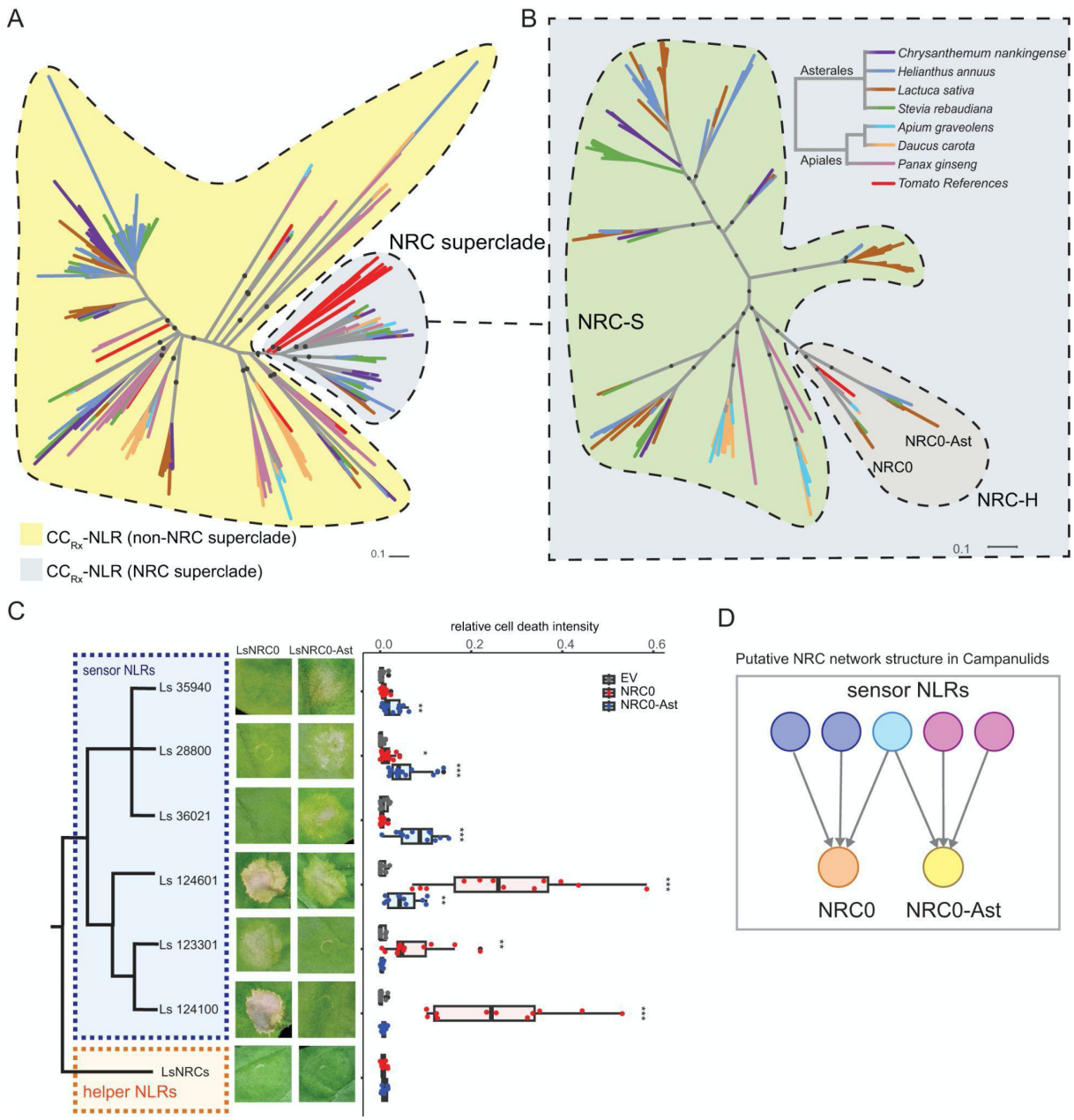

Figure 3. Campanulids show an NRC network with two partially redundant NRC nodes. **A)** Phylogenetic analysis of CC_{Rx}-CNLs from 7 species of campanulids, including *C. nankingense*, *H. annuus*, *L. sativa*, *S. rebaudiana*, *A. graveolens*, *D. carota*, and *P. ginseng*. **B)** Phylogenetic analysis of the NRC superclade from 7 species of campanulids using tomato NRC0 as references. Major branches with bootstrap values > 70 are indicated with black dots in both (A) and (B). **C)** Cell death assay results of NRC-dependent sensor NLRs co-expressed with the lettuce NRCs in *N. benthamiana* at 5 dpi. All sensor NLRs carried the MHD motif (D to V) mutation. As controls, helper NLR LsNRCs (LsNRC0 or LsNRC0-Ast) were infiltrated without sensor NLRs. The dot plot represents the cell death quantification analysed by UVP ChemStudio PLUS. Statistical differences were examined by paired Student's t-test (* = $p < 0.05$, ** = $p < 0.01$, *** = $p < 0.001$, **** = $p < 0.0001$). **D)** Putative NRC network structure in campanulids where some NRC-S signal through NRC0, some NRC-S signal through NRC0-Ast, and some signal through both NRCs to induce HR.

332 NLRs of lettuce are divided into the NRC0-dependent and NRC0-Ast-dependent groups, with
333 some sensor NLRs capable of signalling through both NRCs (Fig. 3, C and D). Altogether, these

334 results suggest that, in campanulids, some orders such as Apiales (carrot) harbour a simple NRC
335 network composed of NRC0 and matching sensor NLRs, whereas the NRC network in other orders
336 such as Asterales (lettuce) contain at least two partially redundant NRCs, namely NRC0 and
337 NRC0-Ast, and the matching sensor NLRs (Fig. 3D).

338 To gain insight into the interchangeability of NRC networks across different species of
339 campanulids, we conducted cross-species comparisons using NRC helper and sensor NLR from
340 both carrot and lettuce. We found that two lettuce sensor NLRs (Ls36021^{DV}, and Ls124601^{DV})
341 trigger cell death when co-expressed with DcNRC0 (Supplemental Fig. S5, A and B). The sensor
342 NLR Ls28800^{DV} triggered weak cell death when co-expressed with DcNRC0, though
343 quantification using image-based analysis was not statistically significant (Supplemental Fig. S5,
344 A and B). Although lettuce NRC0-dependent sensor NLRs (Ls124041^{DV} and Ls123301^{DV}) trigger
345 cell death when co-expressed with LsNRC0, they did not trigger cell death when co-expressed
346 with DcNRC0. Interestingly, carrot sensor NLR Dc23560^{DV}, which induces cell death together
347 with DcNRC0, triggers cell death with both LsNRC0 and LsNRC0-Ast (Supplemental Fig. S5, C
348 and D). These results revealed that DcNRC0, LsNRC0 and LsNRC0-Ast are partially
349 interchangeable, displaying some compatibility with sensor NLRs across the two species.

350 **The NRC network of lamiids is highly expanded**

351 To compare the NRC superclade of different lamiids, we selected 5 lamiids species, including
352 *Erythranthe guttata*, *Fraxinus excelsior*, *Coffea canephora*, *Solanum lycopersicum*, and *I. triloba*,
353 and generated a phylogenetic tree encompassing their NRC superclade members. This tree showed
354 that, within the NRC superclade, the NRC-H clade was the only well-supported clade that
355 contained NLR sequences from all five species (Fig. 4A). Most of the well-supported NRC-S
356 clades only contained sequences from single species. This is consistent with the view that helper
357 NLRs are relatively conserved whereas sensor NLRs have massively diversified in different plant
358 lineages. Further phylogenetic analyses revealed that the NRC family is also highly diverse, with
359 only NRC0 from the five selected species forming a well-supported clade (Fig. 4B). The other
360 NRCs across the five species were rarely found to cluster together, indicating that the NRC family
361 has extensively diversified across different lamiids species.

362 Our data suggests that the NRC superclade is massively expanded in *I. batatas*, *I. triloba*, *I. trifida*
363 of the *Ipomoea* genus (Fig. 1A). We sought to reconstitute the *Ipomoea* NRC network using
364 sequences identified from *I. triloba*, however, we failed to validate the gene models of many of
365 the predicted NLRs using a local *I. triloba* accession. Despite having few NRC members, water
366 spinach (*I. aquatica*) contained representative NRC sequences in each subclade in the phylogenetic
367 tree of the *Ipomoea* NRC superclade (Supplemental Fig. S6A). We, therefore, focused on *I.*
368 *aquatica* for further analysis, aiming to use it as a representative species for validating the genetic
369 structure of the *Ipomoea* NRC network.

370

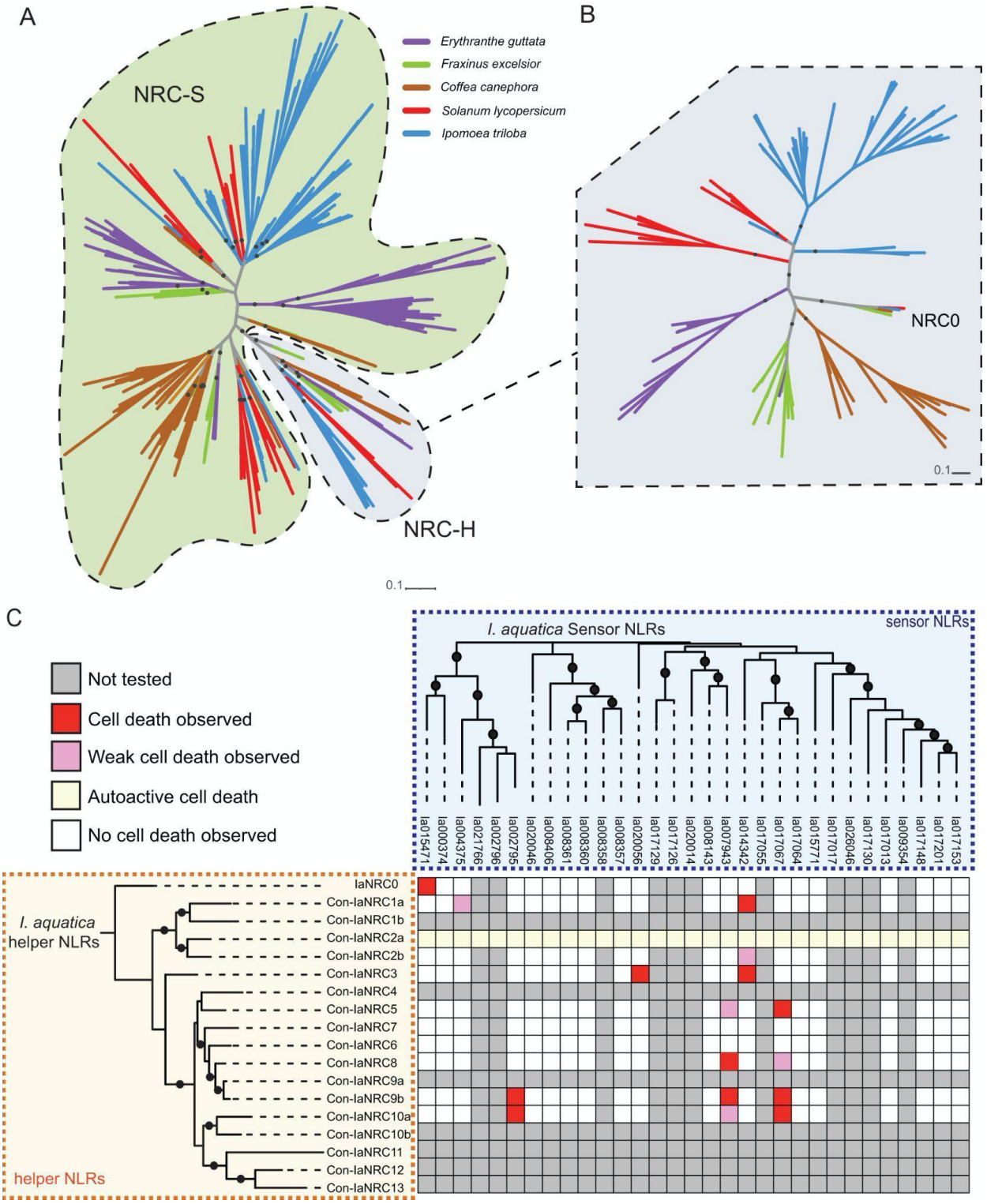

Figure 4. The *Ipomoea* genus possesses a complex NRC network. **A)** Phylogenetic analysis of the NRC superclade of five plant species of lamiids. **B)** Phylogenetic analysis of the NRC family members across five plant species of lamiids. Major branches with bootstrap values > 70 are indicated with black dots in both (A) and (B). **C)** Cell death matrix of *I. aquatica* putative NRC sensor NLRs co-expressed with NRC helper NLRs. All sensor NLRs carried the MHD motif (D to V) mutation. Detailed cell death assay results are provided in Supplemental Fig. S7.

371

372 The *I. aquatica* NRC superclade consists of 18 NRCs and 31 sensor NLRs (Fig. 4C). Since most
373 of these NRCs are not orthologous to the previously described solanaceous NRCs, we name these
374 18 NRCs Convolvulaceae(Con)-IaNRCs to differentiate them from NRCs identified from the
375 Solanaceae (Sol). In addition to the IaNRC0, some of the Con-IaNRCs are located in gene clusters
376 together with putative NRC-S (Supplemental Fig. S6, B and C). We successfully cloned 11 NRCs
377 and 20 putative NRC-S from *I. aquatica* and performed cell death assays as described previously.
378 As expected, the sensor NLR Ia15471^{DV} induced cell death when co-expressed with its physically
379 linked helper NLR, IaNRC0, but not with other Con-IaNRCs (Fig. 4C and Supplemental Fig. S7).
380 An additional 15 sensor NLR and Con-IaNRC pairings were shown to function together,
381 displaying strong or weak cell death when co-expressed in *N. benthamiana* (Fig. 4C and
382 Supplemental Fig. S7). These results indicate that the NRC network in *Ipomoea* exhibits a complex
383 genetic structure, where multiple NRCs are present, showing varying degrees of genetic
384 redundancy similar to the phenomenon observed in Solanaceae (Supplemental Fig. S8).

385 **Family-specific NRC subclades of lamiids show features of diversifying selection**

386 To gain further insights into the evolution of NRC helper NLRs across asterids, we performed
387 phylogenetic analyses using full-length NRC sequences, with the tomato NRC0-dependent sensor
388 NLR (Sl08230) as an outgroup. This phylogenetic tree classified the NRCs into the NRC0
389 subclades (NRC0, NRC0-Eri, NRC0-Ast) and several lineage-specific NRC subclades of lamiids,
390 consistent with the previous analysis using only the NB-ARC domain (Fig. 5A, Supplemental Fig.
391 S9, and Supplemental Fig. S2). In lamiids, the NRC subclades grouped together in a manner
392 largely consistent with their respective family taxonomy (Fig. 5A, Supplemental Fig. S9, and
393 Supplemental Fig. S2). Consequently, we referred to these clusters as family-specific NRC
394 subclades. Next, we performed an adaptive branch-site REL test for episodic diversification
395 (aBSREL), and found signatures of diversifying selection in several of the lamiids family-specific
396 NRC subclades, but not in the NRC0 subclades (Fig. 5A, Supplemental Fig. S9, and Supplemental
397 Data Set 3). Furthermore, NRC0 subclades showed shorter branch lengths in general, whereas the
398 family-specific NRC subclades showed more variable and longer branch lengths (Fig. 5, B and C).
399 These results suggest that the NRC0 subclades are relatively conserved across asterids, while the
400 family-specific NRC subclades have diversified in several lamiids species.

401 **NRC0 subclades across asterids are partially interchangeable**

402 To test the degree to which members of the NRC0 subclades (NRC0, NRC0-Eri, and NRC0-Ast)
403 are interchangeable, we conducted cell death experiments using NRC0 homologs cloned from *C.*
404 *sinensis* (tea), *D. carota* (carrot), *L. sativa* (lettuce), *S. lycopersicum* (tomato), *I. aquatica* (water
405 spinach). We found that tea NRC0-dependent sensor NLR Cs24074^{DV} triggered clear cell death
406 when co-expressed with DcNRC0 and SlNRC0, weak cell with IaNRC0, but no cell death with
407 LsNRC0 or LsNRC0-Ast (Fig. 6, A and D). Out of the two carrot NRC0-dependent sensor NLRs,
408 only one (Dc23650^{DV}) induced cell death when co-expressed with LsNRC0, LsNRC0-Ast,

409 IaNRC0, and SlNRC0 (Fig. 6, B and D). The lettuce NRC0-Ast-dependent sensor NLRs
410 Ls28800^{DV}, Ls35940^{DV} and Ls36021^{DV}, which did not induce cell death when expressed with
411 LsNRC0, induced cell death when co-expressed with NRC0 from the other species (Fig. 6, C and
412 D). The lettuce NRC0-dependent sensor NLRs Ls123301^{DV} and Ls124100^{DV} failed to induce cell
413 death with any of the tested NRC0 variants. Interestingly, the lettuce NRC-S Ls124601^{DV}, which
414 can signal through both LsNRC0 and LsNRC0-Ast, is the only NRC-S that activates cell death
415 with all NRC0 variants tested (Fig. 6, C and D). The water spinach sensor NLR Ia15471^{DV} only
416 induced cell death with SlNRC0 or IaNRC0 but not any of the other tested NRC0 variants.

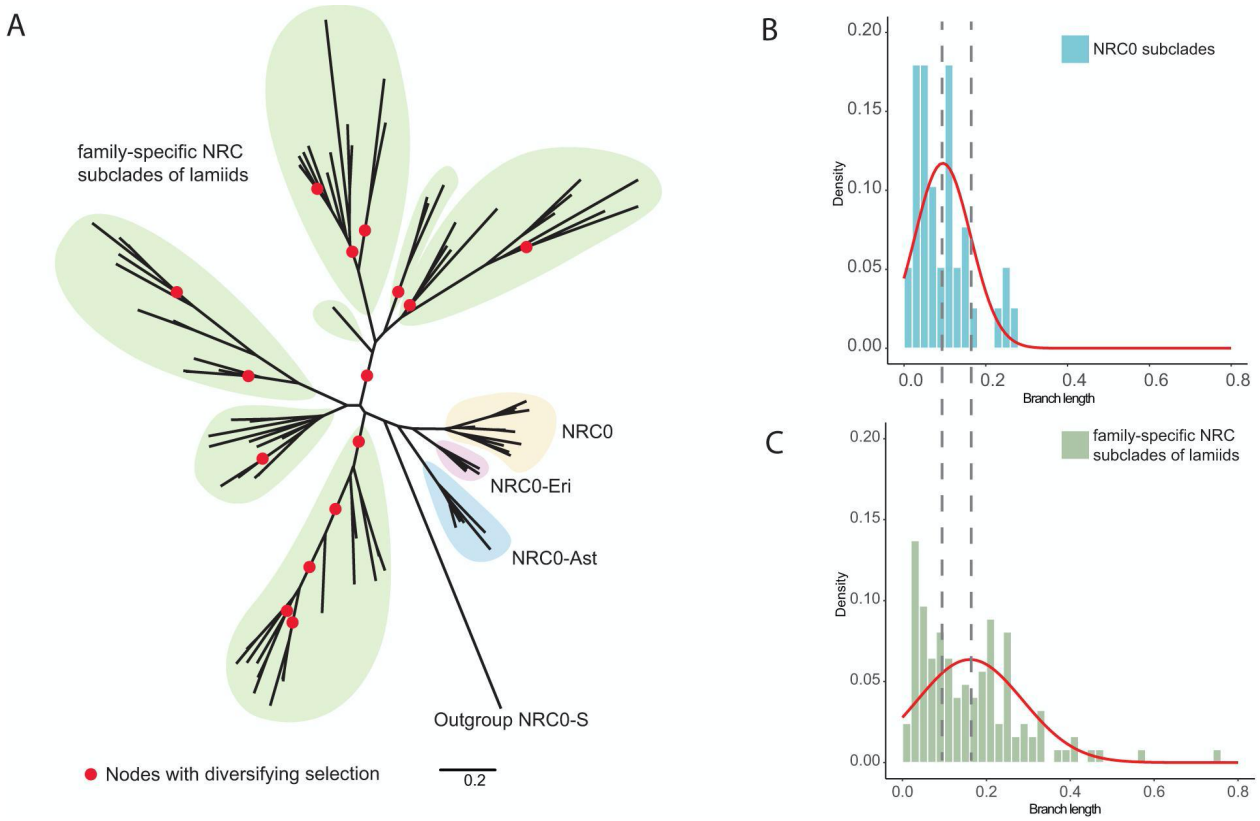

Figure 5. Lamiids family-specific NRC subclades, but not the three NRC0 subclades, show diversifying selection. **A)** Phylogenetic tree based on the full-length sequences of the NRC family from 15 selected asterids species. The aBSREL analysis indicated that 15 out of 81 selected internal branches show episodic diversifying selection. Diversifying selection on branch nodes was assessed using the Likelihood Ratio Test with a significance threshold set at $p \leq 0.05$. Detailed phylogeny and results of aBSREL analysis are provided in Supplemental Fig. S9 and Supplemental Data Set 3. **B)** and **C)** Branch length distribution of the three NRC0 subclades and family-specific NRC subclades of lamiids based on the phylogenetic tree in (A). The red lines in both histograms indicate the predicted normal distribution.

417 Similarly, the tomato NRC0-dependent sensor NLR Sl08230^{DV} only induced cell death with
418 IaNRC0 or SlNRC0 (Fig. 6, C and D). These results indicate that NRC0 homologs exhibit partial
419 interchangeability across different lineages of asterids. Together these results suggest that the
420 NRC0 network, across different asterids lineages, is broadly conserved, however, some of the
421 sensor or helper NLRs have diversified and lost their compatibility with each other (Fig. 6D).

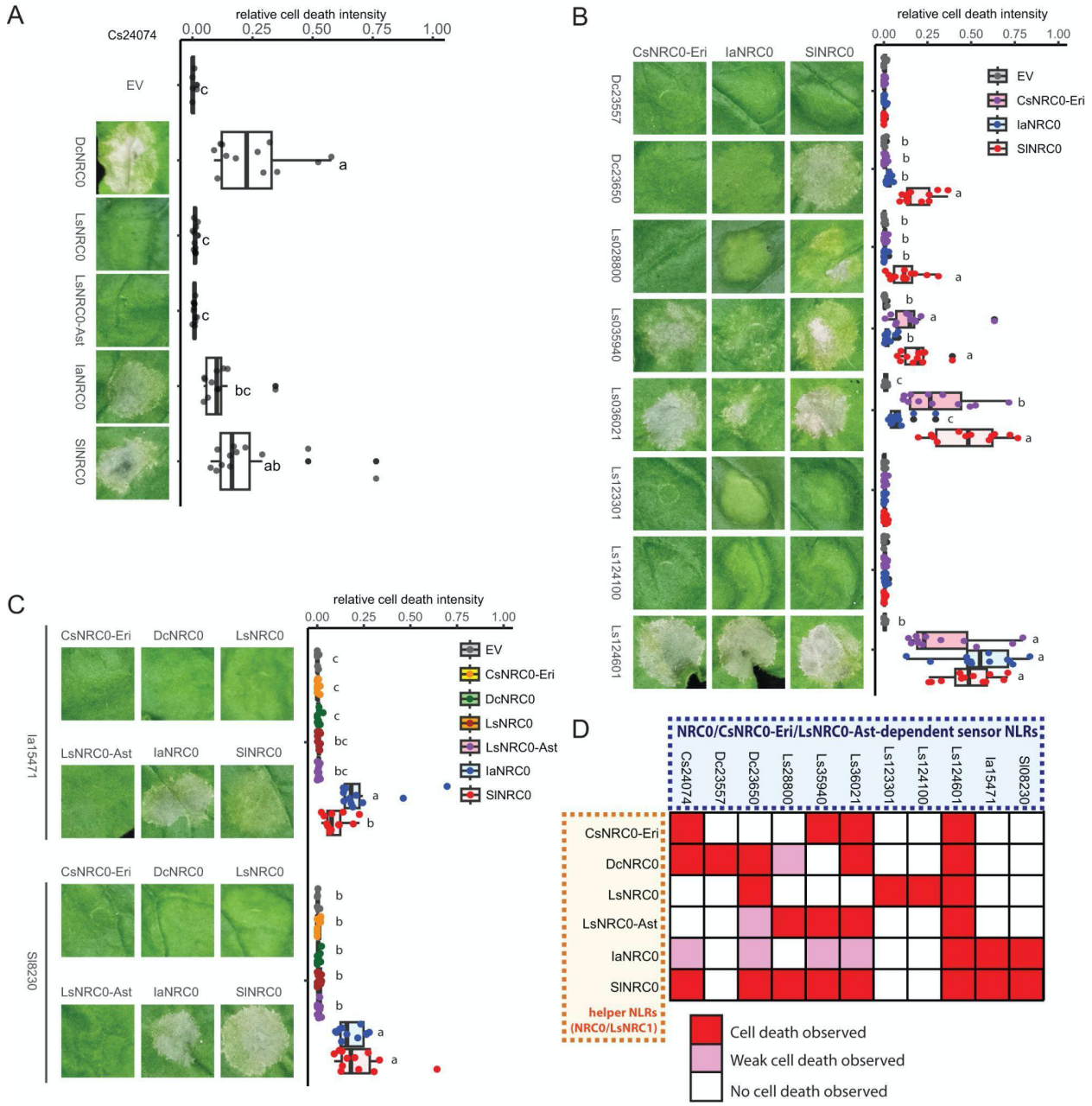

Figure 6. NRC0 subclades from different plant lineages showed varying degrees of interchangeability. **A)** Cell death assay results of tea Cs24074 co-expressed with DcNRC0, LsNRC0, LsNRC0-Ast, IaNRC0, and SlNRC0 in *N. benthamiana* observed at 5 dpi. **B)** Cell death assay results of carrot sensor NLRs (Dc23557 and Dc23650) or lettuce sensor NLRs (Ls28800, Ls35940, Ls36021, Ls123301, Ls124100, and Ls124601) co-expressed with CsNRC0-Eri, IaNRC0, and SlNRC0 in *N. benthamiana* observed at 5 dpi. **C)** Cell death assay results of water spinach sensor NLR (Ia15471) or tomato sensor NLR (Sl08230) co-expressed with CsNRC0-Eri, DcNRC0, LsNRC0, LsNRC0-Ast, IaNRC0, and SlNRC0 in *N. benthamiana* observed at 5 dpi. All sensor NLRs carried the MHD motif (D to V) mutation. The dot plot represents cell death quantification analysed by UVP ChemStudio PLUS. Statistical differences among the samples were analysed with Tukey's HSD test ($p < 0.05$) for each sensor NLR independently. **D)** Matrix of cell death assays of NRC0-dependent sensor NLRs co-expressed with NRC0 homologs from 5 different species of various lineages, including the information obtained from Fig. 2, Fig. 3, Supplemental Fig. S3 and Supplemental Fig. S5.

424 **Sensor and helper NLRs from Solanaceae and Convolvulaceae display some inter-family**
425 **cross-compatibility**

426 We previously characterised the NRC network of Solanaceae, which consists of conserved NRC
427 homologs across most solanaceous plants (Wu et al., 2017). However, phylogenetic analyses of
428 the NRC superclade here revealed that NRC network members have diversified, and expanded
429 extensively in different families of lamiids (Fig. 4, A and B, and Fig. 5A). This has led us to
430 speculate that sensor and helper NLRs of NRC networks from distinct families in lamiids may
431 share very little or no compatibility. To test this, we co-expressed sensor NLRs from solanaceous
432 plants with NRCs from water spinach (representing the Convolvulaceae family), and sensor NLRs
433 from water spinach with NRCs from tomato (representing the Solanaceae family). As expected,
434 most of the solanaceous NLRs, including Bs2, R1, Prf (Pto/AvrPto), and Rpi-blb2, did not trigger
435 cell death when co-expressed with any water spinach NRCs tested (Supplemental Fig. S10 and
436 S11). To our surprise, Rx and Rx2 triggered cell death when co-expressed with Con-IaNRC3, 5,
437 8, and 9, with varying degrees of intensity (Fig. 7, A and B), and Rpi-amr1 triggered cell death
438 when co-expressed with Con-IaNRC9 (Fig. 7, A and B). When we tested the reverse combinations,
439 we found that most of the water spinach sensor NLRs failed to induce cell death with the Sol-
440 SlNRCs tested (Supplemental Fig. S12 and S13). In addition to Ia15471^{DV}, which we previously
441 showed to signal through Sol-SlNRC0, three other water spinach sensor NLRs (Ia04375^{DV},
442 Ia14342^{DV}, and Ia17067^{DV}) also induced cell death (Fig. 7, C and D). Interestingly, all three water
443 spinach sensor NLRs signalled through Sol-SlNRC1 but not the other Sol-SlNRCs tested. This
444 suggests that, despite having family-specific NRC networks, some cross-compatibility between
445 sensor and helper NLRs exists between Solanaceae and Convolvulaceae.

446

447 **Discussion**

448 The NRC network plays an essential role in disease resistance to multiple pathogens of
449 solanaceous plants (Wu et al., 2017). Nevertheless, functional studies of the NRC network beyond
450 solanaceous plants remained limited. We explored the evolutionary diversity of NRC networks
451 across lineages of angiosperms, with a particular focus on the three major lineages of asterids
452 (Ericales, campanulids, and lamiids). These lineages displayed distinct hierarchical structures
453 within their respective NRC networks (Fig. 8). Ericales represents one of the early branches of
454 asterids, predating the divergence of campanulids and lamiids. In our study, tea (*C. sinensis*) served
455 as a representative of Ericales and possessed a relatively simple NRC network. This network
456 involves the transmission of signals from NRC0-Eri-dependent sensor NLRs through NRC0-Eri
457 to induce cell death. Since the three examined Ericales species contained few NRC superclade
458 members, the NRC network in Ericales has likely undergone limited changes over millions of
459 years of evolution (Fig. 8). In campanulids, we identified two partially redundant NRC nodes:
460 NRC0 that is present in both Apiales and Asterales, and NRC0-Ast that exists exclusively to
461 Asterales (Fig. 8). We speculate that NRC0-Ast may have either emerged early in campanulids

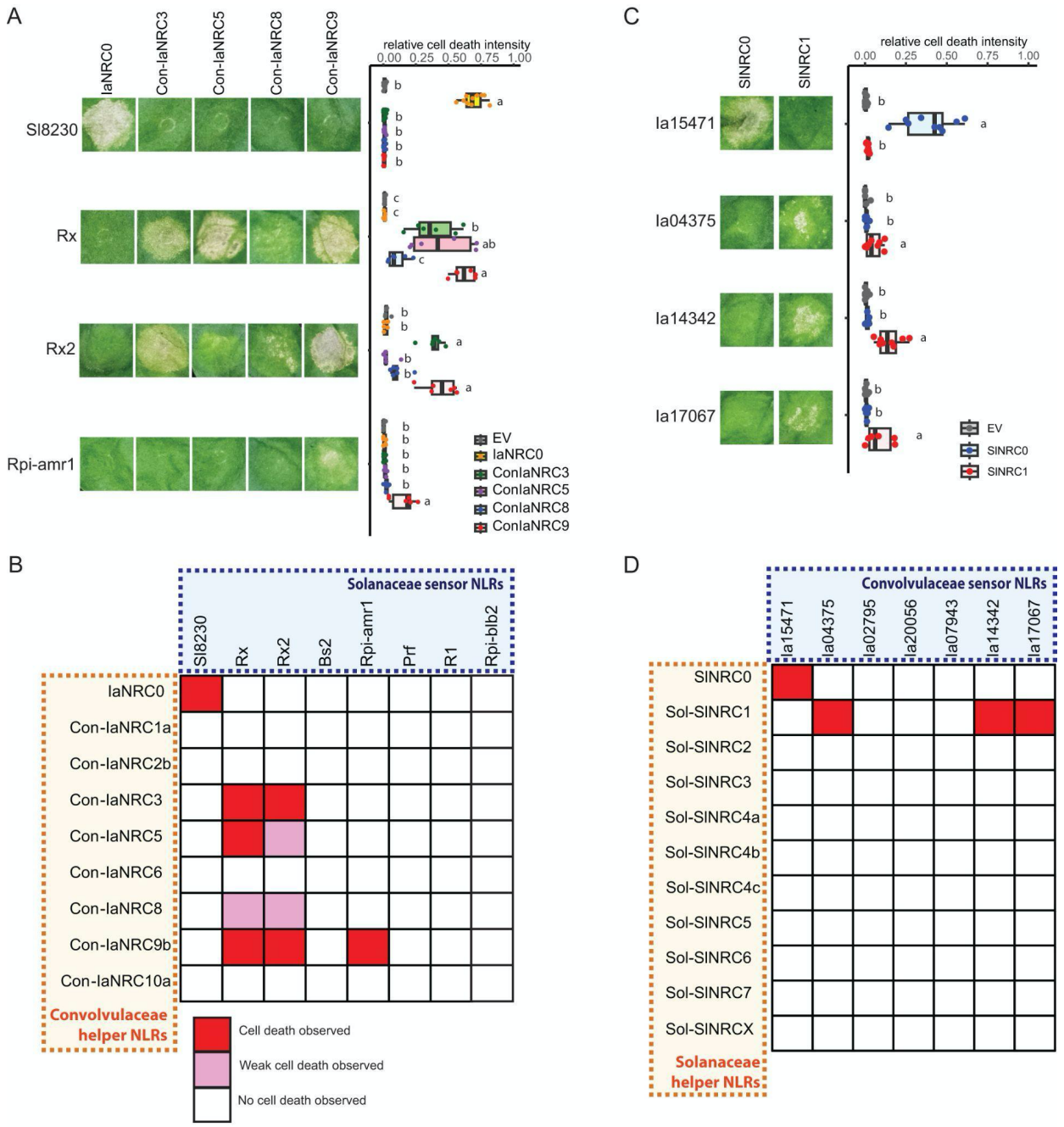

Figure 7. Sensor and helper NLRs in Solanaceae and Convolvulaceae exhibit a degree of cross-compatibility between these two plant families. **A)** Cell death assay results of solanaceous sensor NLRs (Sl8230, Rx, Rx2, and Rpi-amr1) co-expressed with water spinach NRC helpers (IaNRC0, Con-IaNRC3, Con-IaNRC5, Con-IaNRC8, Con-IaNRC9) in *N. benthamiana* at 5 dpi. All sensor NLRs carried the MHD motif (D to V) mutation. The dot plot represents cell death quantification analysed by UVP ChemStudio PLUS. **B)** Matrix of cell death assays for solanaceous NRC-dependent sensor NLRs co-expressed with water spinach NRC helper NLRs, including information obtained from Supplemental Fig. S10 and Supplemental Fig. S11. **C)** Cell death assay results of water spinach sensor NLRs (Ia15471, Ia04375, Ia14342, and Ia17067) co-expressed with solanaceous NRC helpers in *N. benthamiana* at 5 dpi. All sensor NLRs carried the MHD motif (D to V) mutation. The dot plot represents cell death quantification analysed by UVP ChemStudio PLUS. Statistical differences among the samples were analysed with Tukey's HSD test ($p < 0.05$) for each sensor NLR independently. **D)** Matrix of cell death assays for solanaceous NRC-dependent sensor NLRs co-expressed with water spinach NRC helper NLRs, including information obtained from Supplemental Fig. S12 and Supplemental Fig. S13.

462

463 and subsequently been lost in Apiales or arose via duplication of the ancestral NRC0 after the
464 divergence of Asterales and Apiales. The NRC superclade expanded and diversified significantly
465 in most lamiids (Fig. 1, Fig. 5 and Fig. 8). Apart from NRC0 which is very conserved, the
466 phylogenetic tree shows distinct lineage-specific clustering patterns of the NRC family members.
467 This specific diversification pattern appears to be unique for each plant family, implying that the
468 lineage-specific NRC network is likely conserved at the family level (Fig. 5 and Fig. 8). Our results
469 are consistent with the view that the NRC superclade originated from an ancestral NRC sensor-
470 helper pair, and then differentially expanded across plant lineages into complicated immune
471 networks (Wu et al., 2017; Sakai et al., 2023).

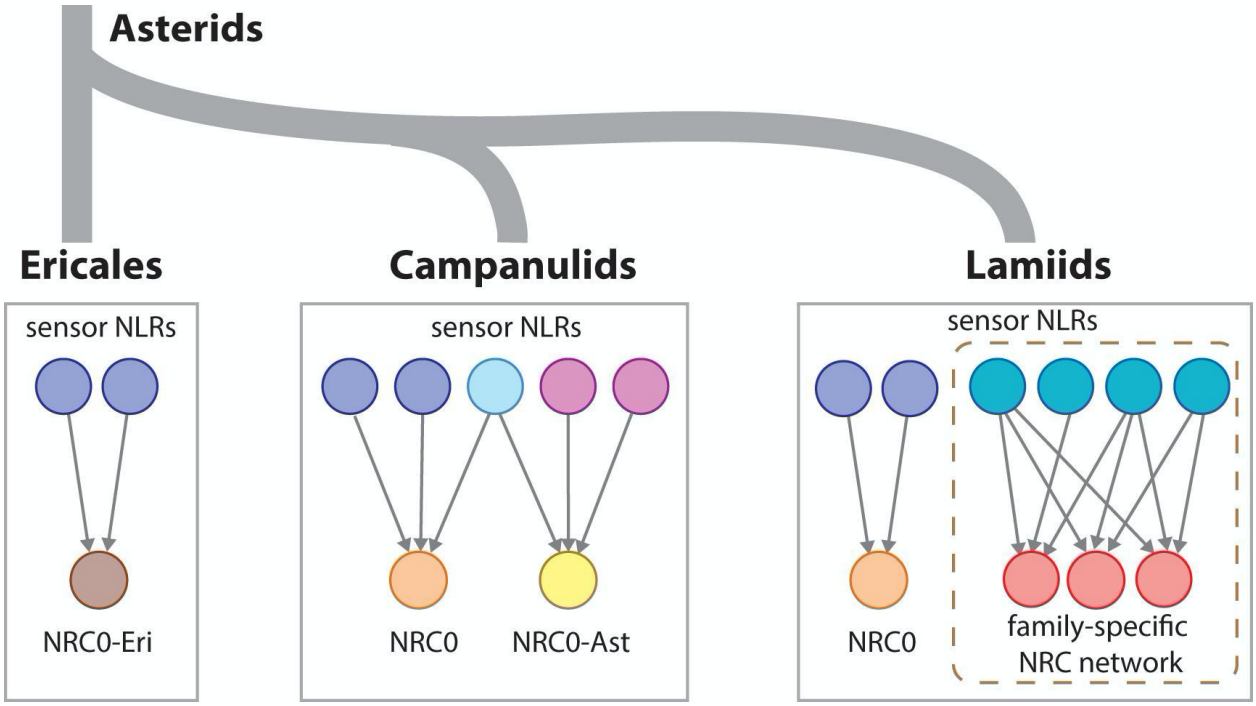

Figure 8. Evolution of the hierarchical structure of the NRC network in asterids. Ericales encode a simple NRC network where few sensor NLRs signal through NRC0-Eri to induce cell death. Campanulids show duplicated NRC nodes where some NRC-S signal through NRC0, some NRC-S signal through NRC0-Ast, and some signal through both NRCs to induce cell death. In addition to NRC0, lamiids display massively expanded and complex NRC networks that are likely plant family-specific.

472 Tandem gene and whole-genome duplication (WGD), genetic drift, relaxed selection during
473 domestication, and adaptation to ecological niches have all been reported to influence the
474 expansion and contraction of *NLR* genes (Han and Tsuda, 2022). While the total number of protein-
475 coding genes shows a weak correlation with the expansion of NLRs, it is even more weakly
476 correlated with the expansion of the NRC superclade (Fig. 1B and Supplemental Fig. S1) (Baggs
477 et al., 2017; Borrelli et al., 2018). *Capsicum annuum*, for example, has a large number of NRC
478 superclade members despite having relatively few total protein-coding genes (Fig. 1A and
479 Supplemental Data Set 2) (Seo et al., 2016). Conversely, ginseng has high total protein-coding
480 gene numbers but few NRC superclade members (Fig. 1A and Supplemental Data Set 2). Selection
481 pressures placed on each plant lineage in asterids may, therefore, have led to distinct expansion or

482 contraction patterns of the NRC superclade. Furthermore, the evolutionary events leading to the
483 expansion of the NRC superclade show no correlation to the overall genome size (Supplemental
484 Fig. S1). Since the massive expansion of the NRC superclade is a unique feature observed in
485 lamiids, we speculate that selection pressure in the ancestral lamiids species may have led to the
486 initial expansion of the NRC network. This ancient expansion provided advantages for the species
487 to survive and was further selected independently in the subsequent lamiids progenies. While most
488 lamiids species encode large numbers of NRC superclade members, *E. ulmoides* stands out as the
489 only lamiids species analysed that does not have NLRs belonging to the NRC superclade (Fig. 1A).
490 Although we have not yet been able to exclude the possibility that this is due to the insufficient
491 quality of the assembled genome. Additional genome information from related species may help
492 address whether early gene loss events led to the absence of the NRC superclade in this species.
493 Notably, 89% of NLRs predicted from the parasitic plant *S. asiatica* were classified within the
494 NRC superclade, whereas *Cuscuta* spp., and many other parasitic plants, have undergone
495 substantial loss of their NLRs (Fig. 1A) (Baggs et al., 2020; Liu et al., 2021). It would be interesting
496 to understand whether and how the unique lifestyle of these and other parasitic plants may have
497 differentially shaped the overall evolution of plant immunity, including the NRC superclade.

498 NLR genes are frequently located within gene clusters which can serve as a repository of genetic
499 variation. Most of these clusters are results of tandem duplication leading to homogeneous NLR
500 clusters, while heterogenous clusters are less prominent (Jupe et al., 2012; Meyers et al., 2005;
501 Zhou et al., 2004). NRC0 stands out as the most conserved NRC homolog among asterids (Sakai
502 et al., 2023). Furthermore, the NRC0 sensor-helper NLR gene cluster was identified in several
503 species, representing the ancestral state of the NRC network (Sakai et al., 2023). We proposed that
504 breaking the physical linkage between sensor and helper NLRs was critical to enable the
505 independent evolution of both sensor and helper NLRs (Wu et al., 2017; Leister, 2004). However,
506 we noticed that, in several cases, sensor NLRs that are unlinked to NRC0 accumulated mutations
507 leading to loss-of-function or truncation. For example, in Ericales, most of the sensor NLRs of the
508 NRC superclade appeared to be truncated, and only those linked to NRC0-Eri retained full-length
509 NLR sequence signatures (Fig. 2 and Supplemental Fig. S2). A similar phenomenon was observed
510 in carrots (campanulids), where only the sensor NLRs that were closely linked to NRC0 remained
511 functional (Supplemental Fig. S3). In lettuce, all the sensor NLRs that signal through NRC0 are
512 located on the same chromosome as NRC0 (Supplemental Fig. S4). Interestingly, the sensor NLRs
513 that signal through NRC0-Ast are located on chromosomes different from NRC0-Ast. The three
514 sensor NLRs that signal through NRC0-Ast show longer branch lengths in the phylogenetic tree
515 compared to the NRC0-dependent sensor NLRs (Supplemental Fig. S4A). This suggests that, after
516 becoming physically unlinked from their helper NLR partners, the sensor NLRs are indeed more
517 prone to accumulating mutations, leading to diversification or non-functionalisation (Leister, 2004;
518 Baumgarten et al., 2003). In water spinach, we identified a few sensor-helper NLR clusters in
519 addition to the NRC0 cluster (Supplemental Fig. S6). One of the sensor NLRs (Ia014342) is
520 capable of signalling through its linked NRC (Con-IaNRC1b), as well as two other NRCs located
521 on different chromosomes. Similar to what was observed in solanaceous crops, most of the NRC

522 superclade members are dispersed on different chromosomes, forming a few gene clusters (Wu et
523 al., 2017; Seo et al., 2016). These results suggest that the expansion of the NRC superclade
524 coincides with the transposition and tandem duplication of both sensor and helper NLR genes
525 independently. Transposable elements, particularly the long terminal repeat retrotransposons, were
526 shown to contribute to the tandem duplication and transposition of NLR genes in plant genomes
527 (Wei et al., 2002; Kim et al., 2017; Seidl and Thomma, 2017; Hao et al., 2023). Whether the
528 associations with transposable elements correlate with the expansion of the NRC superclade in
529 different plant lineages requires further investigation.

530 The NRC superclade likely originated from an ancient sensor-helper NLR cluster that contained a
531 one-to-one or two-to-one ratio of sensor and helper NLRs (Wu et al., 2017; Sakai et al., 2023).
532 Our results indicate that NRC-S duplicated more times than NRC-Hs in most species analysed and
533 generally showed longer branch lengths than that of helper NLRs in the phylogenetic trees (Fig.
534 1C, Fig. 2A, Fig. 3A, and Fig. 4A). This is consistent with the view that sensor NLRs are often
535 under high dynamic and balancing selection, whereas helper NLRs show slower evolution rates
536 and remain functionally conserved (Stam et al., 2019; Shimizu et al., 2022; Seo et al., 2016).
537 Furthermore, an expanded and diversified sensor NLR repertoire offers a higher potential for
538 conferring resistance to pathogens (Barragan and Weigel, 2021). In campanulids, where the NRC
539 superclade is not as extensively expanded, certain species such as *S. rebaudiana* encode a high
540 sensor-to-helper ratio (Fig. 1C). This is perhaps due to several tandem duplication and
541 transposition events that occurred to NRC-S but not to NRC-H in these species. Although sensor
542 NLRs are generally highly expanded in lamiids, leading to a high sensor-to-helper ratio, *I. cairica*,
543 *I. aquatica*, and *N. benthamiana* are among the few species in which the sensor-to-helper ratio
544 remains close to the ancestral ratio (Fig. 1C). One possible explanation is that NLR contraction
545 contributes to the reduction of the sensor-to-helper ratio, with many of sensor NLRs being lost
546 during evolution. NLR contraction events have been reported in lineages of Brassicaceae and
547 Apiaceae species (Luo et al., 2012; Shao et al., 2014; Zhang et al., 2016; Shao et al., 2016; Liang
548 and Dong, 2023). Additional macroevolutionary analyses with diverse plant genomes may provide
549 insights into how NLR expansion and contraction events influence sensor-helper NLR ratios and
550 provide information on the factors that drive NLR contraction.

551 NRC0 stands out as the most conserved NRC across different plant lineages (Sakai et al., 2023).
552 We found two other NRC0 subclades, namely NRC0-Eri and NRC0-Ast, which show partial
553 interchangeability with the NRC0 clade defined by Sakai et al. (2023) (Fig. 6). The three NRC0
554 subclades show relatively short branch lengths, indicating that NRC0 homologs have not
555 undergone significant diversification since its split from the ancestral species (Fig. 5). Recent
556 macroevolutionary studies of ZAR1 homologs revealed that ZAR1 is the most conserved NLR
557 across angiosperms and evolved to function with partnered RLCKs early in its evolutionary history
558 (Adachi et al., 2023b; Harant et al., 2022). While RLCKs rapidly diversified to keep pace with
559 fast-evolving effectors, ZAR1 experienced relatively limited expansion and duplication (Adachi
560 et al., 2023b). Whether the conservation of NRC0 subclades is due to its critical role in immunity

561 or simply a lack of pathogen pressure remains to be investigated. The phylogenetic tree of the NRC
562 family in lamiids indicated that, apart from the highly conserved NRC0s, there are no clear
563 orthologous NRCs across different plant families (Fig. 4B, and Fig. 5A). Nevertheless, some NRC-
564 S from solanaceous plants can activate some *Ipomoea* NRCs to induce cell death, and some NRC-
565 S from *I. aquatica* are capable of inducing cell death through SlNRC1 (Fig. 7). Therefore, while
566 NRCs function as helper NLRs that mediate cell death for NRC-S, this group of genes has
567 diversified to an extent that functional orthologs (such as NRC0) are rarely found in plants from
568 different families. Despite this, compatibility between sensor and helper NLR across different
569 plant families has been observed (e.g. between Solanaceae and Convolvulaceae). Further studies
570 focusing on understanding the molecular mechanisms underpinning these interactions may help
571 elucidate the critical changes that determine compatibility between NRCs and their matching
572 sensor NLRs.

573 Our findings reveal the overall diversity and hierarchical structure of NRC networks in plants
574 belonging to different lineages of asterids. Except for a small number of NRC-H that can cooperate
575 with NRC-S from different plant lineages, the majority of NRC-H do not function with NRC-S
576 from divergent plant species. Knowledge of sensor-helper compatibility may be particularly useful
577 for overcoming restricted taxonomic functionality, a challenge when transferring resistance genes
578 across distantly related plants (Tai et al., 1999; Narusaka et al., 2013). In the cases of NLRs
579 belonging to the NRC network, it may be necessary to transfer both the matching sensor and helper
580 NLRs together. The recent discovery that CaRpi-blb2 specifically signals through the pepper
581 helper NLRs CaNRC8 and CaNRC9 further emphasizes the importance of understanding the
582 commonalities and differences in the immunity networks of various related species (Oh et al.,
583 2023). Among the *Ipomoea* species, *I. trifida, I. tiloba,* and *I. batatas* encode high numbers of
584 overall NLRs in their genomes. Given that the majority of NLRs in these three species belong to
585 the NRC superclade, delving into the NRC network of *Ipomoea* species might offer opportunities
586 to utilize their NLRome as a resource for conferring disease resistance against a variety of
587 pathogens. Further investigations into the evolution of the NRC network, along with validation
588 using NRC-Ss that confer resistance in combination with their corresponding NRCs, could
589 increase the likelihood of successfully transferring disease resistance across distantly related crops.

590

591 **Materials and methods**

592 **Prediction and phylogenetic analyses of NLRs**

593 The annotated protein sequences of selected plant species used in this study were downloaded from
594 public databases (Supplemental Data Set 1). To identify the proteins containing the NB-ARC
595 domain, sequences were scanned with MAST in MEME v 5.4.0 using 20 previously defined motifs
596 with default parameters (Bailey et al., 2009; Jupe et al., 2012). The NB-ARC domains with at least
597 three of the four major motifs (P-loop, GLPL, Kinase2 and MHD) and a length of at least 150

598 residues were considered intact. Sequences with truncated NB-ARC domains were excluded from
599 further analyses. Full-length NLR sequences were aligned using MAFFT version 7 using the G-
600 INS-1 progressive method with default settings (Katoh et al., 2019). The aligned amino acid
601 sequences were imported into MEGA 7 for manual trimming leaving only the NB-ARC domain
602 for phylogenetic analysis. Phylogenetic trees were constructed using Maximum-likelihood
603 phylogenetic analyses using the evolutionary model JTT+G+I with 200 bootstrap tests.
604 Phylogenetic trees were further processed and visualized using FigTree and iTOL (Kumar et al.,
605 2016; Rambaut, 2021; Letunic and Bork, 2021). NLR sequences from tomato were included as
606 references for the identification of the NRC superclade. The species tree of angiosperms in Fig. 1
607 was modified from the published phylogenetic tree (The Angiosperm Phylogeny Group, 2016).

608 **Detection of positive selection**

609 Full-length nucleotide sequences of the NRC family were analysed using MEGA 7. The nucleotide
610 sequences were translated into protein sequences and subsequently aligned using ClustalW. Gaps
611 in the alignment were manually removed. The resulting trimmed amino acid sequences of the NRC
612 family were subjected to phylogenetic analyses. Phylogenetic trees were constructed using
613 Maximum-likelihood phylogenetic analyses with the evolutionary model JTT+G+I and 200
614 bootstrap tests. The aligned NRC family amino acid sequences were reversed-translated into
615 nucleotide sequences. Along with the phylogenetic tree, alignment of the nucleotide sequences of
616 the NRC family was subjected to aBSREL (An adaptive branch-site REL test for episodic
617 diversification) using the HyPhy (Hypothesis testing using Phylogenies) package on the
618 Datamonkey Adaptive Evolution Server (https://www.datamonkey.org/) (Smith et al., 2015;
619 Weaver et al., 2018; Kosakovsky Pond et al., 2020). SlNRC0-dependent sensor NLR Sl8230
620 (Solyc10g008230) was included as an outgroup.

621 **RNA and DNA isolation**

622 Materials of carrot (*Daucus carota*), kiwifruits (*Actinidia chinensis*), tea (*Camelia sinensis*),
623 lettuce (*Lactuca sativa*), and water spinach (*Ipomoea aquatica*) were obtained from local nurseries
624 or grocery stores. *Ipomoea triloba* was collected from the campus of Academia Sinica (Nankang,
625 Taipei, Taiwan) and confirmed by Sanger sequencing using ITK and MatK primers. DNA was
626 extracted from young seedlings or mature leaves using DNeasy Plant Mini Kit (Qiagen). RNA was
627 extracted using Plant Total RNA Mini Kits (VIOGENE). Synthesis of cDNA was performed using
628 SuperScript™ III Reverse Transcriptase (Invitrogen) following the manufacturer's instructions.

629 **Cloning of NLR genes**

630 Full-length NLRs were amplified from genomic DNA or cDNA with primers designed based on
631 the available genome sequences. The PCR amplicons were cloned into the pAGM9121 (Addgene
632 plasmid #51833), pICH41308 (Addgene plasmid #47998) using Golden Gate Cloning (Weber et
633 al., 2011) or pTA in T&A™ Cloning Kit from Yeastern Biotech (Taiwan). The putative sensor

634 NLRs of tea (Cs0021741 and Cs0024074), *I. aquatica* NRC6, and Rx2 were synthesized in
635 pUC57-Kan as MoClo level 0 modules using the service provided by SynBio Technologies (New
636 Jersey, USA). Mutations (D to V) of the MHD motif were carried out using inverse PCR with
637 primers containing AarI (NEB) or BsmBI (NEB) enzyme sites for digestion followed by ligation
638 using T4 DNA ligase (Invitrogen). The constructs were then subcloned into binary vector
639 pICSL86922OD using BsaI (NEB) and T4 DNA ligase (Invitrogen). pICSL86922OD was kindly
640 provided by Mark Youles (The Sainsbury Laboratory, UK) (Addgene plasmid # 86181). The NLR
641 gene expression constructs were then transformed into *Agrobacterium tumefaciens* (GV3101)
642 using electroporation. The NLR gene sequences and cloning primers used in this research are listed
643 in Supplemental Data Set 4 and Supplemental Data Set 5. Several previously described NRC-
644 dependent solanaceous NLRs (R), including R1, Rx, Rpi-amr1, Rpi-blb2, Bs2, and Prf (Pto), and
645 the corresponding effectors, including AVR1, CP, AVRamr1, AVRblb2, AvrBs2, and AvrPto
646 were used in the cell death assays together with Con-IaNRCs (Wu et al., 2017; Lin et al., 2022).

647 **Agroinfiltration and quantification of cell death in *N. benthamiana* leaves**

648 Transient expression of NLRs were performed on 4-week-old *N. benthamiana* leaves (WT or
649 *nrc2/3/4*_KO) with *A. tumefaciens* (GV3101) carrying the indicated expression constructs (Wu et
650 al., 2020; Witek et al., 2021). *A. tumefaciens* suspensions in infiltration buffer (10 mM MES, 10
651 mM MgCl2, and 150 µM acetosyringone, pH 5.6) were adjusted to suitable OD_{600} and then
652 infiltrated into *N. benthamiana* leaves using needleless syringes. The agro-infiltrated plants were
653 kept in a walk-in growth chamber (temperature 24-26°C, humidity 45–65% and 16/8 hr light/dark
654 cycle) for 5 days before imaging and autofluorescence-based cell death quantification using UVP
655 ChemStudio PLUS (Analytik Jena). Raw cell death autofluorescence images were acquired using
656 blue LED light for excitation and the FITC filter (513 - 557 nm) as the emission filter. Areas
657 showing stronger visual cell death generally produce stronger autofluorescence at this wavelength
658 range. The exposure time was adjusted to 10 seconds to avoid saturation of the autofluorescence
659 signal. The mean signal intensity was calculated using VisionWorks v.11.2 software by manually
660 selecting the infiltrated areas and subtracting the background signal intensity. The mean signal
661 intensity value was further normalized with the maximum intensity (65535) to obtain the relative
662 intensity of cell death. Results of cell death assays were presented as relative cell death intensity
663 from at least 6 technical replicates. Paired t-test was used for comparisons between two groups
664 using the rstatix package in R studio (Kassambara, 2023). ANOVA followed by Tukey's HSD test
665 was used to perform multiple comparisons using the multcompView package in R studio software
666 (Graves and Dorai-Raj, 2023). $P<0.05$ was considered to be with statistically significant
667 differences. In some cases, co-expression of the NRC-H and NRC-S induces visible cell death but
668 quantification using image-based analysis was not statistically significant. We classified this as
669 weak cell death to differentiate it from the no visible cell death phenotype observed.

670 **Acknowledgements**

We thank Dr. Sophien Kamoun (The Sainsbury Laboratory, UK), Dr. Hiroaki Adachi (Laboratory of Crop Evolution, Graduate School of Agriculture, Kyoto University) and Toshiyuki Sakai (Laboratory of Crop Evolution, Graduate School of Agriculture, Kyoto University) for valuable suggestions on the research and comments on the manuscript. We thank Mark Youles (SynBio, The Sainsbury Laboratory, UK) for sharing plasmids for molecular cloning. We also thank Dr. Chih-Horng Kuo, Dr. Lay-Sun Ma, and Dr. Ting-Ying Wu (Institute of Plant and Microbial Biology, Academia Sinica) for their suggestions on the experimental design and data presentation. C.H.W. is funded by the 2030 Cross-Generation Young Scholars Program of the National Science and Technology Council, Taiwan (NSTC 112-2628-B-001-007). L.D. is funded by a National Institute of Agricultural Botany (NIAB) Fellowship. Research in the LD lab is supported by the British Society of Plant Pathology, the Gatsby Charitable Foundation and the Royal Society.

Author Contributions

F.J.G. and C.H.W. designed the research. F.J.G. and C.Y.H. conducted the experiments. F.J.G. analysed the data. F.J.G., L.D., and C.H.W. wrote the manuscript.

690 **References**
691
692 **Adachi, H., Contreras, M.P., Harant, A., Wu, C.-H., Derevnina, L., Sakai, T., Duggan, C.,**
693 **Moratto, E., Bozkurt, T.O., Maqbool, A., Win, J., and Kamoun, S.** (2019). An N-
694 terminal motif in NLR immune receptors is functionally conserved across distantly
695 related plant species. eLife **8**: e49956.
696 **Adachi, H., Sakai, T., Harant, A., Pai, H., Honda, K., Toghani, A., Claeys, J., Duggan, C.,**
697 **Bozkurt, T.O., Wu, C.-H., and Kamoun, S.** (2023a). An atypical NLR protein
698 modulates the NRC immune receptor network in *Nicotiana benthamiana*. PLoS Genet.
699 **19**: e1010500.
700 **Adachi, H., Sakai, T., Kourelis, J., Pai, H., Gonzalez Hernandez, J.L., Utsumi, Y., Seki, M.,**
701 **Maqbool, A., and Kamoun, S.** (2023b). Jurassic NLR: conserved and dynamic
702 evolutionary features of the atypically ancient immune receptor ZAR1. Plant Cell:
703 koad175.
704 **Ahn, H., Lin, X., Olave-Achury, A.C., Derevnina, L., Contreras, M.P., Kourelis, J., Wu, C.,**
705 **Kamoun, S., and Jones, J.D.G.** (2023). Effector-dependent activation and
706 oligomerization of plant NRC class helper NLRs by sensor NLR immune receptors Rpi-
707 amr3 and Rpi-amr1. EMBO J. **42**: e111484.
708 **Andolfo, G., Di Donato, A., Chiaiese, P., De Natale, A., Pollio, A., Jones, J.D.G., Frusciante,**
709 **L., and Ercolano, M.R.** (2019). Alien domains shaped the modular structure of plant
710 NLR proteins. Genome Biol. Evol. **11**: 3466–3477.
711 **Ashikawa, I., Hayashi, N., Yamane, H., Kanamori, H., Wu, J., Matsumoto, T., Ono, K., and**
712 **Yano, M.** (2008). Two adjacent nucleotide-binding site-leucine-rich repeat class genes
713 are required to confer Pikm-specific rice blast resistance. Genetics **180**: 2267–2276.
714 **Baggs, E.L., Monroe, J.G., Thanki, A.S., O'Grady, R., Schudoma, C., Haerty, W., and**
715 **Krasileva, K.V.** (2020). Convergent loss of an EDS1/PAD4 signaling pathway in several
716 plant lineages reveals coevolved components of plant immunity and drought response.
717 Plant Cell **32**: 2158–2177.
718 **Bailey, T.L., Boden, M., Buske, F.A., Frith, M., Grant, C.E., Clementi, L., Ren, J., Li,**
719 **W.W., and Noble, W.S.** (2009). MEME SUITE: tools for motif discovery and searching.
720 Nucleic Acids Res. **37**: W202-208.
721 **Barragan, A.C. and Weigel, D.** (2021). Plant NLR diversity: the known unknowns of pan-
722 NLRomes. Plant Cell **33**: 814–831.
723 **Baumgarten, A., Cannon, S., Spangler, R., and May, G.** (2003). Genome-level evolution of
724 resistance genes in *Arabidopsis thaliana*. Genetics **165**: 309–319.
725 **Bi, G. et al.** (2021). The ZAR1 resistosome is a calcium-permeable channel triggering plant
726 immune signaling. Cell **184**: 3528-3541 e12.
727 **Castel, B., Ngou, P.-M., Cevik, V., Redkar, A., Kim, D.-S., Yang, Y., Ding, P., and Jones,**
728 **J.D.G.** (2019). Diverse NLR immune receptors activate defence via the RPW8-NLR
729 NRG1. New Phytol. **222**: 966–980.
730 **Cesari, S. et al.** (2013). The rice resistance protein pair RGA4/RGA5 recognizes the
731 *Magnaporthe oryzae* effectors AVR-Pia and AVR1-CO39 by direct binding. Plant Cell
732 **25**: 1463–1481.
733 **Cesari, S., Kanzaki, H., Fujiwara, T., Bernoux, M., Chalvon, V., Kawano, Y., Shimamoto,**
734 **K., Dodds, P., Terauchi, R., and Kroj, T.** (2014). The NB-LRR proteins RGA4 and
735 RGA5 interact functionally and physically to confer disease resistance. EMBO J. **33**:

1941–1959.
Chen, Z., Wu, Q., Tong, C., Chen, H., Miao, D., Qian, X., Zhao, X., Jiang, L., and Tao, X. (2021). Characterization of the Roles of SGT1/RAR1, EDS1/NDR1, NPR1, and NRC/ADR1/NRG1 in Sw-5b-Mediated Resistance to *Tomato Spotted Wilt Virus*. Viruses **13**: 1447.
Chia, K.-S., Kourelis, J., Vickers, M., Sakai, T., Kamoun, S., and Carella, P. (2022). The N-terminal executioner domains of NLR immune receptors are functionally conserved across major plant lineages. bioRxiv: 2022.10.19.512840.
Collier, S.M., Hamel, L.-P., and Moffett, P. (2011). Cell death mediated by the N-terminal domains of a unique and highly conserved class of NB-LRR protein. Mol. Plant-Microbe Interact. **24**: 918–931.
Contreras, M.P. et al. (2023a). Sensor NLR immune proteins activate oligomerization of their NRC helpers in response to plant pathogens. EMBO J. **42**: e111519.
Contreras, M.P., Lüdke, D., Pai, H., Toghani, A., and Kamoun, S. (2023b). NLR receptors in plant immunity: making sense of the alphabet soup. EMBO Rep. **24**:e57495.
Dodds, P.N. and Rathjen, J.P. (2010). Plant immunity: towards an integrated view of plant–pathogen interactions. Nat. Rev. Genet. **11**: 539–548.
Duxbury, Z., Wu, C., and Ding, P. (2021). A comparative overview of the intracellular guardians of plants and animals: NLRs in innate immunity and beyond. Annu. Rev. Plant Biol. **72**: 155–184.
Ence, D., Smith, K.E., Fan, S., Gomide Neves, L., Paul, R., Wegrzyn, J., Peter, G.F., Kirst, M., Brawner, J., Nelson, C.D., and Davis, J.M. (2022). NLR diversity and candidate fusiform rust resistance genes in loblolly pine. G3 **12**: jkab421.
Förderer, A. et al. (2022). A wheat resistosome defines common principles of immune receptor channels. Nature **610**: 532–539.
Gao, Y., Wang, W., Zhang, T., Gong, Z., Zhao, H., and Han, G.-Z. (2018). Out of Water: The Origin and Early Diversification of Plant *R* -Genes. Plant Physiol. **177**: 82–89.
Graves, S. and Dorai-Raj, H.-P.P. and L.S. with help from S. (2023). multcompView: Visualizations of Paired Comparisons. https://cran.r-project.org/web/packages/multcompView/index.html
Han, X. and Tsuda, K. (2022). Evolutionary footprint of plant immunity. Curr. Opin. Plant Biol. **67**: 102209.
Hao, Y., Pan, Y., Chen, W., Rashid, M.A.R., Li, M., Che, N., Duan, X., and Zhao, Y. (2023). Contribution of Duplicated Nucleotide-Binding Leucine-Rich Repeat (NLR) Genes to Wheat Disease Resistance. Plants **12**: 2794.
Harant, A., Pai, H., Sakai, T., Kamoun, S., and Adachi, H. (2022). A vector system for fast-forward studies of the HOPZ-ACTIVATED RESISTANCE1 (ZAR1) resistosome in the model plant *Nicotiana benthamiana*. Plant Physiol. **188**: 70–80.
International Wheat Genome Sequencing Consortium et al. (2018). Chromosome-scale comparative sequence analysis unravels molecular mechanisms of genome dynamics between two wheat cultivars. Genome Biol. **19**: 104.
Jacob, F., Vernaldi, S., and Maekawa, T. (2013). Evolution and Conservation of Plant NLR Functions. Front. Immunol. **4**:297.
Jones, J.D.G., Vance, R.E., and Dangl, J.L. (2016). Intracellular innate immune surveillance devices in plants and animals. Science **354**: aaf6395.
Jupe, F., Pritchard, L., Etherington, G.J., Mackenzie, K., Cock, P.J.A., Wright, F., Sharma,

782 **S.K., Bolser, D., Bryan, G.J., Jones, J.D.G., and Hein, I.** (2012). Identification and
783 localisation of the NB-LRR gene family within the potato genome. BMC Genomics **13**:
784 75.
785 **Kassambara, A.** (2023). rstatix: Pipe-Friendly Framework for Basic Statistical Tests.
786 https://CRAN.R-project.org/package=rstatix
787 **Katoh, K., Rozewicki, J., and Yamada, K.D.** (2019). MAFFT online service: multiple
788 sequence alignment, interactive sequence choice and visualization. Brief. Bioinform. **20**:
789 1160–1166.
790 **Kim, S. et al.** (2017). New reference genome sequences of hot pepper reveal the massive
791 evolution of plant disease-resistance genes by retroduplication. Genome Biol. **18**: 210.
792 **Kosakovsky Pond, S.L. et al.** (2020). HyPhy 2.5—A Customizable Platform for Evolutionary
793 Hypothesis Testing Using Phylogenies. Mol. Biol. Evol. **37**: 295–299.
794 **Kourelis, J., Contreras, M.P., Harant, A., Pai, H., Lüdke, D., Adachi, H., Derevnina, L.,**
795 **Wu, C.-H., and Kamoun, S.** (2022). The helper NLR immune protein NRC3 mediates
796 the hypersensitive cell death caused by the cell-surface receptor Cf-4. PLOS Genet. **18**:
797 e1010414.
798 **Kourelis, J., Sakai, T., Adachi, H., and Kamoun, S.** (2021). RefPlantNLR is a comprehensive
799 collection of experimentally validated plant disease resistance proteins from the NLR
800 family. PLOS Biol. **19**: e3001124.
801 **Kourelis, J. and Van Der Hoorn, R.A.L.** (2018). Defended to the Nines: 25 Years of
802 Resistance Gene Cloning Identifies Nine Mechanisms for R Protein Function. Plant Cell
803 **30**: 285–299.
804 **Kuang, H., Woo, S.-S., Meyers, B.C., Nevo, E., and Michelmore, R.W.** (2004). Multiple
805 genetic processes result in heterogeneous rates of evolution within the major cluster
806 disease resistance genes in lettuce. Plant Cell **16**: 2870–2894.
807 **Kumar, S., Stecher, G., and Tamura, K.** (2016). MEGA7: Molecular Evolutionary Genetics
808 Analysis Version 7.0 for Bigger Datasets. Mol. Biol. Evol. **33**: 1870–1874.
809 **Lee, H., Mang, H., Choi, E., Seo, Y., Kim, M., Oh, S., Kim, S., and Choi, D.** (2021).
810 Genome-wide functional analysis of hot pepper immune receptors reveals an autonomous
811 NLR clade in seed plants. New Phytol. **229**: 532–547.
812 **Leister, D.** (2004). Tandem and segmental gene duplication and recombination in the evolution
813 of plant disease resistance gene. Trends Genet. **20**: 116–122.
814 **Letunic, I. and Bork, P.** (2021). Interactive Tree Of Life (iTOL) v5: an online tool for
815 phylogenetic tree display and annotation. Nucleic Acids Res. **49**: W293–W296.
816 **Liang, X. and Dong, J.** (2023). Comparative-genomic analysis reveals dynamic NLR gene loss
817 and gain across Apiaceae species. Front. Genet. **14**: 1141194.
818 **Lin, X. et al.** (2022). A potato late blight resistance gene protects against multiple *Phytophthora*
819 species by recognizing a broadly conserved RXLR-WY effector. Mol. Plant **15**: 1457–
820 1469.
821 **Liu, Y., Zeng, Z., Zhang, Y.-M., Li, Q., Jiang, X.-M., Jiang, Z., Tang, J.-H., Chen, D.,**
822 **Wang, Q., Chen, J.-Q., and Shao, Z.-Q.** (2021). An angiosperm NLR Atlas reveals that
823 NLR gene reduction is associated with ecological specialization and signal transduction
824 component deletion. Mol. Plant **14**: 2015–2031.
825 **Luo, S., Zhang, Y., Hu, Q., Chen, J., Li, K., Lu, C., Liu, H., Wang, W., and Kuang, H.**
826 (2012). Dynamic Nucleotide-Binding Site and Leucine-Rich Repeat-Encoding Genes in
827 the Grass Family. Plant Physiol. **159**: 197–210.

828 **Maqbool, A., Saitoh, H., Franceschetti, M., Stevenson, C., Uemura, A., Kanzaki, H.,**
829 **Kamoun, S., Terauchi, R., and Banfield, M.** (2015). Structural basis of pathogen
830 recognition by an integrated HMA domain in a plant NLR immune receptor. eLife **4**:
831 e08709.
832 **Marchal, C., Michalopoulou, V.A., Zou, Z., Cevik, V., and Sarris, P.F.** (2022). Show me
833 your ID: NLR immune receptors with integrated domains in plants. Essays Biochem. **66**:
834 527–539.
835 **Martin, E.C., Ion, C.F., Ifrimescu, F., Spiridon, L., Bakker, J., Goverse, A., and Petrescu,**
836 **A.-J.** (2023). NLRscape: an atlas of plant NLR proteins. Nucleic Acids Res. **51**: 1470–
837 1482.
838 **Meyers, B.C., Kaushik, S., and Nandety, R.S.** (2005). Evolving disease resistance genes. Curr.
839 Opin. Plant Biol. **8**: 129–134.
840 **Michelmore, R.W. and Meyers, B.C.** (1998). Clusters of resistance genes in plants evolve by
841 divergent selection and a birth-and-death process. Genome Res. **8**: 1113–1130.
842 **Narusaka, M., Kubo, Y., Hatakeyama, K., Imamura, J., Ezura, H., Nanasato, Y., Tabei, Y.,**
843 **Takano, Y., Shirasu, K., and Narusaka, Y.** (2013). Breaking restricted taxonomic
844 functionality by dual resistance genes. Plant Signal. Behav. **8**: e24244.
845 **Narusaka, M., Shirasu, K., Noutoshi, Y., Kubo, Y., Shiraishi, T., Iwabuchi, M., and**
846 **Narusaka, Y.** (2009). RRS1 and RPS4 provide a dual Resistance-gene system against
847 fungal and bacterial pathogens. Plant J. **60**: 218–226.
848 **Ngou, B.P.M., Ding, P., and Jones, J.D.G.** (2022). Thirty years of resistance: Zig-zag through
849 the plant immune system. Plant Cell **34**: 1447–1478.
850 **Oh, S., Kim, S., Park, H., Kim, M., Seo, M., Wu, C., Lee, H., Kim, H., Kamoun, S., and**
851 **Choi, D.** (2023). Nucleotide-binding leucine-rich repeat network underlies nonhost
852 resistance of pepper against the Irish potato famine pathogen *Phytophthora infestans*.
853 Plant Biotechnol. J. **21**: 1361–1372.
854 **Ortiz, D. and Dodds, P.N.** (2018). Plant NLR Origins Traced Back to Green Algae. Trends
855 Plant Sci. **23**: 651–654.
856 **Rambaut, A.** (2021). Figtree v1.4.4. http://tree.bio.ed.ac.uk/software/figtree/
857 **Saile, S.C., Jacob, P., Castel, B., Jubic, L.M., Salas-Gonzáles, I., Bäcker, M., Jones, J.D.G.,**
858 **Dangl, J.L., and El Kasmi, F.** (2020). Two unequally redundant "helper" immune
859 receptor families mediate *Arabidopsis thaliana* intracellular "sensor" immune receptor
860 functions. PLOS Biol. **18**: e3000783.
861 **Sakai, T., Martinez-Anaya, C., Contreras, M.P., Kamoun, S., Wu, C.-H., and Adachi, H.**
862 (2023). The NRC0 gene cluster of sensor and helper NLR immune receptors is
863 functionally conserved across asterid plants. bioRxiv: 2023.10.23.563533.
864 **Sarris, P.F. et al.** (2015). A Plant Immune Receptor Detects Pathogen Effectors that Target
865 WRKY Transcription Factors. Cell **161**: 1089–1100.
866 **Seidl, M.F. and Thomma, B.P.H.J.** (2017). Transposable Elements Direct The Coevolution
867 between Plants and Microbes. Trends Genet. **33**: 842–851.
868 **Seo, E., Kim, S., Yeom, S.-I., and Choi, D.** (2016). Genome-Wide Comparative Analyses
869 Reveal the Dynamic Evolution of Nucleotide-Binding Leucine-Rich Repeat Gene Family
870 among Solanaceae Plants. Front. Plant Sci. **7**: 1205.
871 **Seong, K., Seo, E., Witek, K., Li, M., and Staskawicz, B.** (2020). Evolution of NLR resistance
872 genes with noncanonical N-terminal domains in wild tomato species. New Phytol. **227**:
873 1530–1543.

874 **Shao, Z.-Q., Xue, J.-Y., Wang, Q., Wang, B., and Chen, J.-Q.** (2019). Revisiting the Origin of
875 Plant NBS-LRR Genes. Trends Plant Sci. **24**: 9–12.
876 **Shao, Z.-Q., Xue, J.-Y., Wu, P., Zhang, Y.-M., Wu, Y., Hang, Y.-Y., Wang, B., and Chen,**
877 **J.-Q.** (2016). Large-Scale Analyses of Angiosperm Nucleotide-Binding Site-Leucine-
878 Rich Repeat Genes Reveal Three Anciently Diverged Classes with Distinct Evolutionary
879 Patterns. Plant Physiol. **170**: 2095–2109.
880 **Shao, Z.-Q., Zhang, Y.-M., Hang, Y.-Y., Xue, J.-Y., Zhou, G.-C., Wu, P., Wu, X.-Y., Wu,**
881 **X.-Z., Wang, Q., Wang, B., and Chen, J.-Q.** (2014). Long-Term Evolution of
882 Nucleotide-Binding Site-Leucine-Rich Repeat Genes: Understanding Gained from and
883 beyond the Legume Family. Plant Physiol. **166**: 217–234.
884 **Shimizu, M. et al.** (2022). A genetically linked pair of NLR immune receptors shows
885 contrasting patterns of evolution. Proc. Natl. Acad. Sci. U. S. A. **119**: e2116896119.
886 **Smith, M.D., Wertheim, J.O., Weaver, S., Murrell, B., Scheffler, K., and Kosakovsky Pond,**
887 **S.L.** (2015). Less Is More: An Adaptive Branch-Site Random Effects Model for Efficient
888 Detection of Episodic Diversifying Selection. Mol. Biol. Evol. **32**: 1342–1353.
889 **Sohn, K.H., Segonzac, C., Rallapalli, G., Sarris, P.F., Woo, J.Y., Williams, S.J., Newman,**
890 **T.E., Paek, K.H., Kobe, B., and Jones, J.D.G.** (2014). The nuclear immune receptor
891 RPS4 is required for RRS1SLH1-dependent constitutive defense activation in
892 Arabidopsis thaliana. PLoS Genet. **10**: e1004655.
893 **Stam, R., Silva-Arias, G.A., and Tellier, A.** (2019). Subsets of NLR genes show differential
894 signatures of adaptation during colonization of new habitats. New Phytol. **224**: 367–379.
895 **Steuernagel, B., Jupe, F., Witek, K., Jones, J.D.G., and Wulff, B.B.H.** (2015). NLR-parser:
896 rapid annotation of plant NLR complements. Bioinformatics **31**: 1665–1667.
897 **Tai, T.H., Dahlbeck, D., Clark, E.T., Gajiwala, P., Pasion, R., Whalen, M.C., Stall, R.E.,**
898 **and Staskawicz, B.J.** (1999). Expression of the Bs2 pepper gene confers resistance to
899 bacterial spot disease in tomato. Proc. Natl. Acad. Sci. U. S. A. **96**: 14153–14158.
900 **Tarr, D.E.K. and Alexander, H.M.** (2009). TIR-NBS-LRR genes are rare in monocots:
901 evidence from diverse monocot orders. BMC Res. Notes **2**: 197.
902 **Terefe-Ayana, D., Kaufmann, H., Linde, M., and Debener, T.** (2012). Evolution of the Rdr1
903 TNL-cluster in roses and other Rosaceous species. BMC Genomics **13**: 409.
904 **The Angiosperm Phylogeny Group** (2016). An update of the Angiosperm Phylogeny Group
905 classification for the orders and families of flowering plants: APG IV. Bot. J. Linn. Soc.
906 **181**: 1–20.
907 **Upson, J.L., Zess, E.K., Białas, A., Wu, C., and Kamoun, S.** (2018). The coming of age of
908 EvoMPMI: evolutionary molecular plant–microbe interactions across multiple
909 timescales. Curr. Opin. Plant Biol. **44**: 108–116.
910 **Van De Weyer, A.-L., Monteiro, F., Furzer, O.J., Nishimura, M.T., Cevik, V., Witek, K.,**
911 **Jones, J.D.G., Dangl, J.L., Weigel, D., and Bemm, F.** (2019). A Species-Wide
912 Inventory of NLR Genes and Alleles in *Arabidopsis thaliana*. Cell **178**: 1260-1272.e14.
913 **Wang, G. et al.** (2015). The Decoy Substrate of a Pathogen Effector and a Pseudokinase Specify
914 Pathogen-Induced Modified-Self Recognition and Immunity in Plants. Cell Host Microbe
915 **18**: 285–295.
916 **Wang, J., Hu, M., Wang, J., Qi, J., Han, Z., Wang, G., Qi, Y., Wang, H.-W., Zhou, J.-M.,**
917 **and Chai, J.** (2019). Reconstitution and structure of a plant NLR resistosome conferring
918 immunity. Science **364**: eaav5870.
919 **Weaver, S., Shank, S.D., Spielman, S.J., Li, M., Muse, S.V., and Kosakovsky Pond, S.L.**

920 (2018). Datamonkey 2.0: A Modern Web Application for Characterizing Selective and
921 Other Evolutionary Processes. Mol. Biol. Evol. **35**: 773–777.
922 **Weber, E., Engler, C., Gruetzner, R., Werner, S., and Marillonnet, S.** (2011). A modular
923 cloning system for standardized assembly of multigene constructs. PloS One **6**: e16765.
924 **Wei, F., Wing, R.A., and Wise, R.P.** (2002). Genome Dynamics and Evolution of the Mla
925 (Powdery Mildew) Resistance Locus in Barley. Plant Cell **14**: 1903–1917.
926 **Witek, K. et al.** (2021). A complex resistance locus in *Solanum americanum* recognizes a
927 conserved *Phytophthora* effector. Nat. Plants **7**: 198–208.
928 **Wu, C.-H., Abd-El-Haliem, A., Bozkurt, T.O., Belhaj, K., Terauchi, R., Vossen, J.H., and**
929 **Kamoun, S.** (2017). NLR network mediates immunity to diverse plant pathogens. Proc.
930 Natl. Acad. Sci. U. S. A. **114**: 8113–8118.
931 **Wu, C.-H., Adachi, H., De la Concepcion, J.C., Castells-Graells, R., Nekrasov, V., and**
932 **Kamoun, S.** (2020). NRC4 Gene Cluster Is Not Essential for Bacterial Flagellin-
933 Triggered Immunity. Plant Physiol. **182**: 455–459.
934 **Wu, C.H., Belhaj, K., Bozkurt, T.O., Birk, M.S., and Kamoun, S.** (2016). Helper NLR
935 proteins NRC2a/b and NRC3 but not NRC1 are required for Pto-mediated cell death and
936 resistance in *Nicotiana benthamiana*. New Phytol **209**: 1344–52.
937 **Wu, C.-H., Derevnina, L., and Kamoun, S.** (2018). Receptor networks underpin plant
938 immunity. Science **360**: 1300–1301.
939 **Wu, C.H. and Kamoun, S.** (2021). Tomato *Prf* requires NLR helpers *NRC2* and *NRC3* to
940 confer resistance against the bacterial speck pathogen *Pseudomonas syringae* pv. *tomato*.
941 Acta Hortic.: 61–66.
942 **Wu, Z., Tian, L., Liu, X., Zhang, Y., and Li, X.** (2021). TIR signal promotes interactions
943 between lipase-like proteins and ADR1-L1 receptor and ADR1-L1 oligomerization. Plant
944 Physiol. **187**: 681–686.
945 **Xi, Y., Cesari, S., and Kroj, T.** (2022). Insight into the structure and molecular mode of action
946 of plant paired NLR immune receptors. Essays Biochem. **66**: 513–526.
947 **Zhang, Y.-M., Shao, Z.-Q., Wang, Q., Hang, Y.-Y., Xue, J.-Y., Wang, B., and Chen, J.-Q.**
948 (2016). Uncovering the dynamic evolution of nucleotide-binding site-leucine-rich repeat
949 (NBS-LRR) genes in Brassicaceae: Evolution of NBS-LRR genes in Brassicaceae. J.
950 Integr. Plant Biol. **58**: 165–177.
951 **Zhou, T., Wang, Y., Chen, J.-Q., Araki, H., Jing, Z., Jiang, K., Shen, J., and Tian, D.**
952 (2004). Genome-wide identification of NBS genes in japonica rice reveals significant
953 expansion of divergent non-TIR NBS-LRR genes. Mol. Genet. Genomics **271**: 402–415.
954

Supplemental Figures

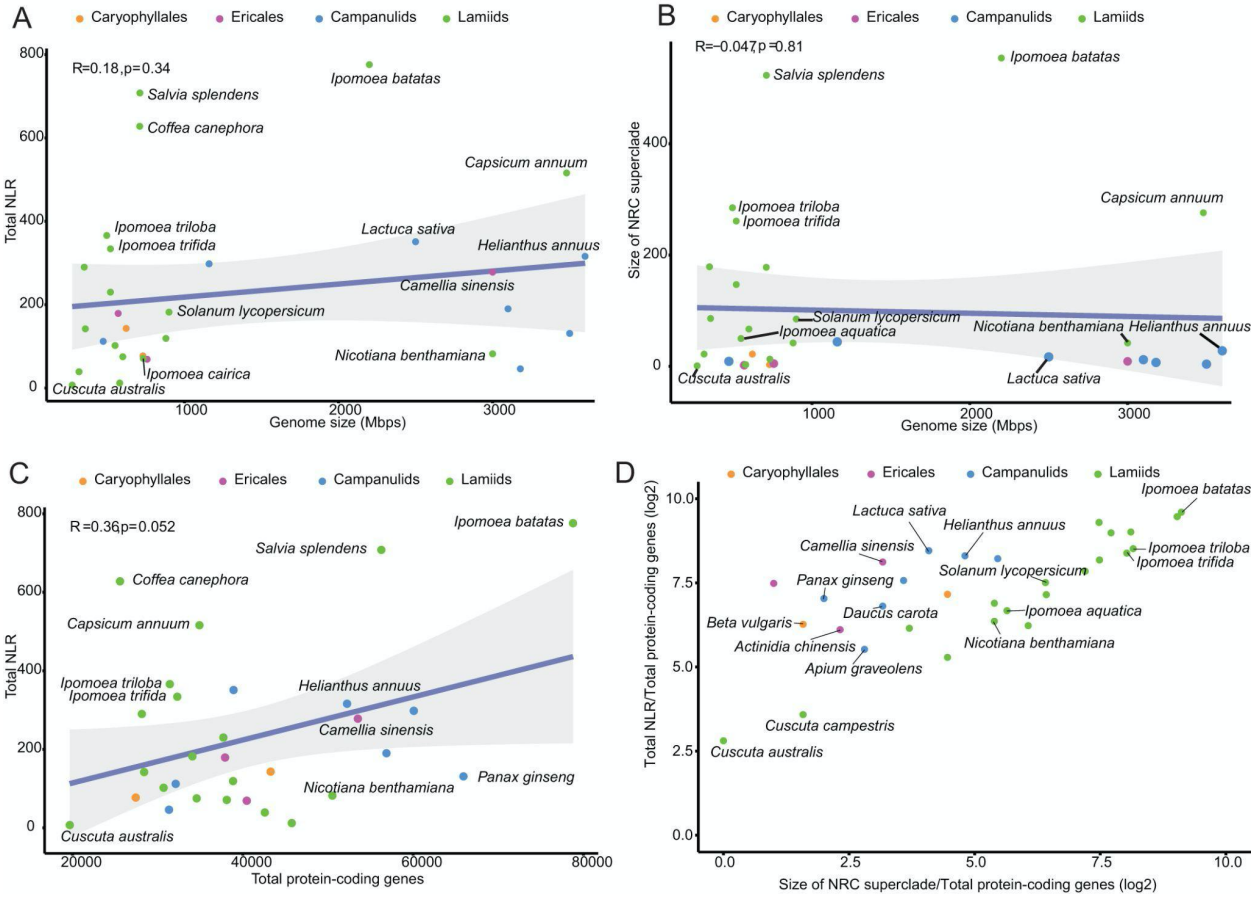

Supplemental Fig. S1. Correlation of the size of total NLRs or NRC superclade with total genome size or total protein-coding genes. **A)** Total NLR and genome size show weak correlations. **B)** The size of the NRC superclade and total protein-coding genes shows no correlation. **C)** Total NLR and total protein-coding gene showed a weak correlation. **D)** Lamiids plant species showed a higher size of NRC superclade from total NLR out of total protein-coding genes (log2). Plant species from different lineages indicated are labelled with different colours.

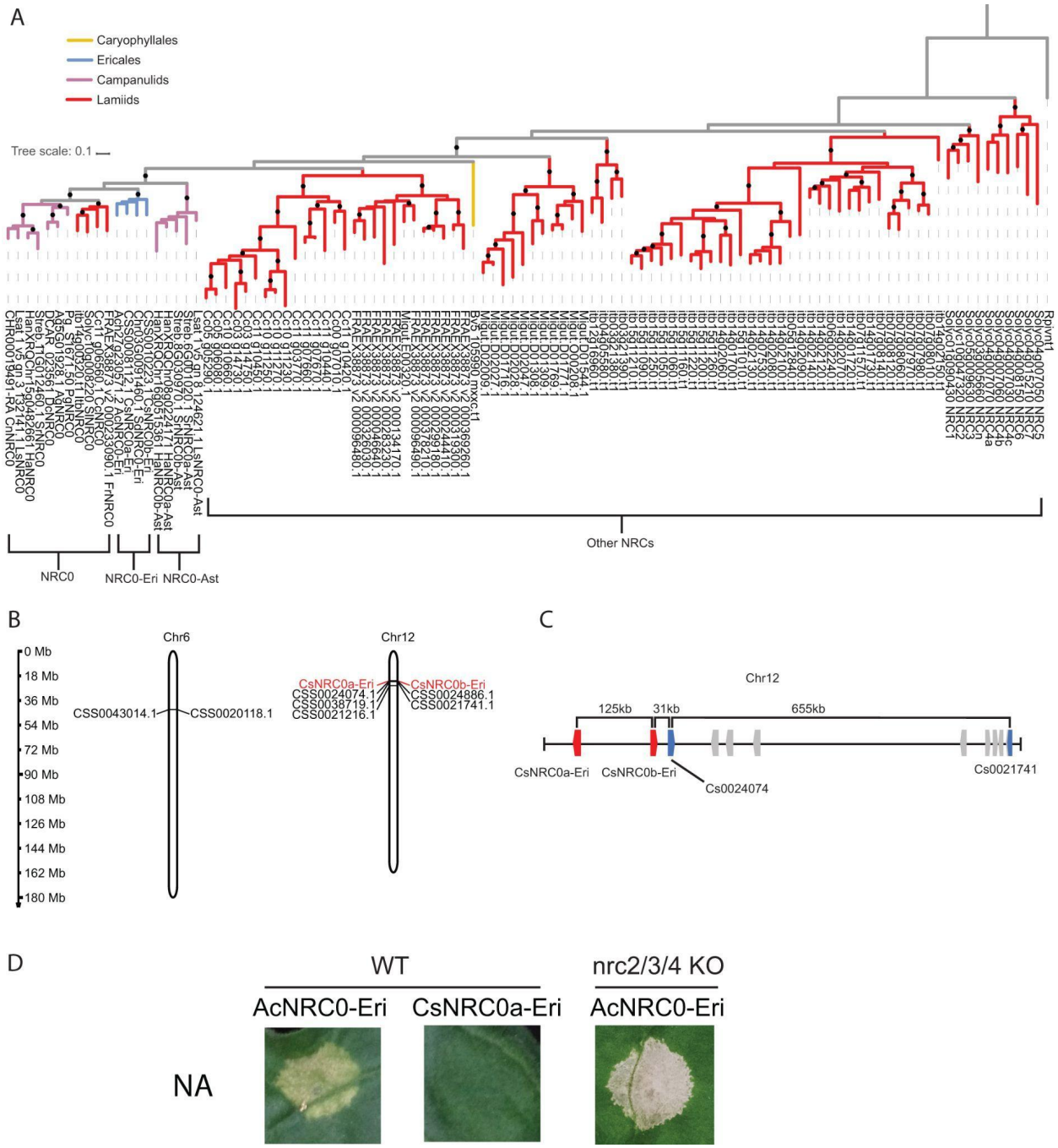

Supplemental Fig. S2. Tea NRC0-Eri and putative sensor NLRs are located in a gene cluster. **A)** Phylogenetic analysis of NRC helpers from Caryophyllales (*B. vulgaris*), Ericales, campanulids and lamiids. Nodes with bootstrap values over 70 are labelled with black dots. **B)** The NRC superclade members of tea (*C. sinensis*) form gene clusters on chromosome 6 and chromosome 12. **C)** The NRC0 sensor and helper genes cluster together on chromosome 12. **D)** The kiwifruit NRC0 exhibited autoactivity when expressed in *N. benthamiana* leaves. "WT" represents Wild type *N. benthamiana* plants, and "nrc2/3/4 KO" represents *nrc2/nrc3/nrc4* triple knockout *N. benthamiana* plants.

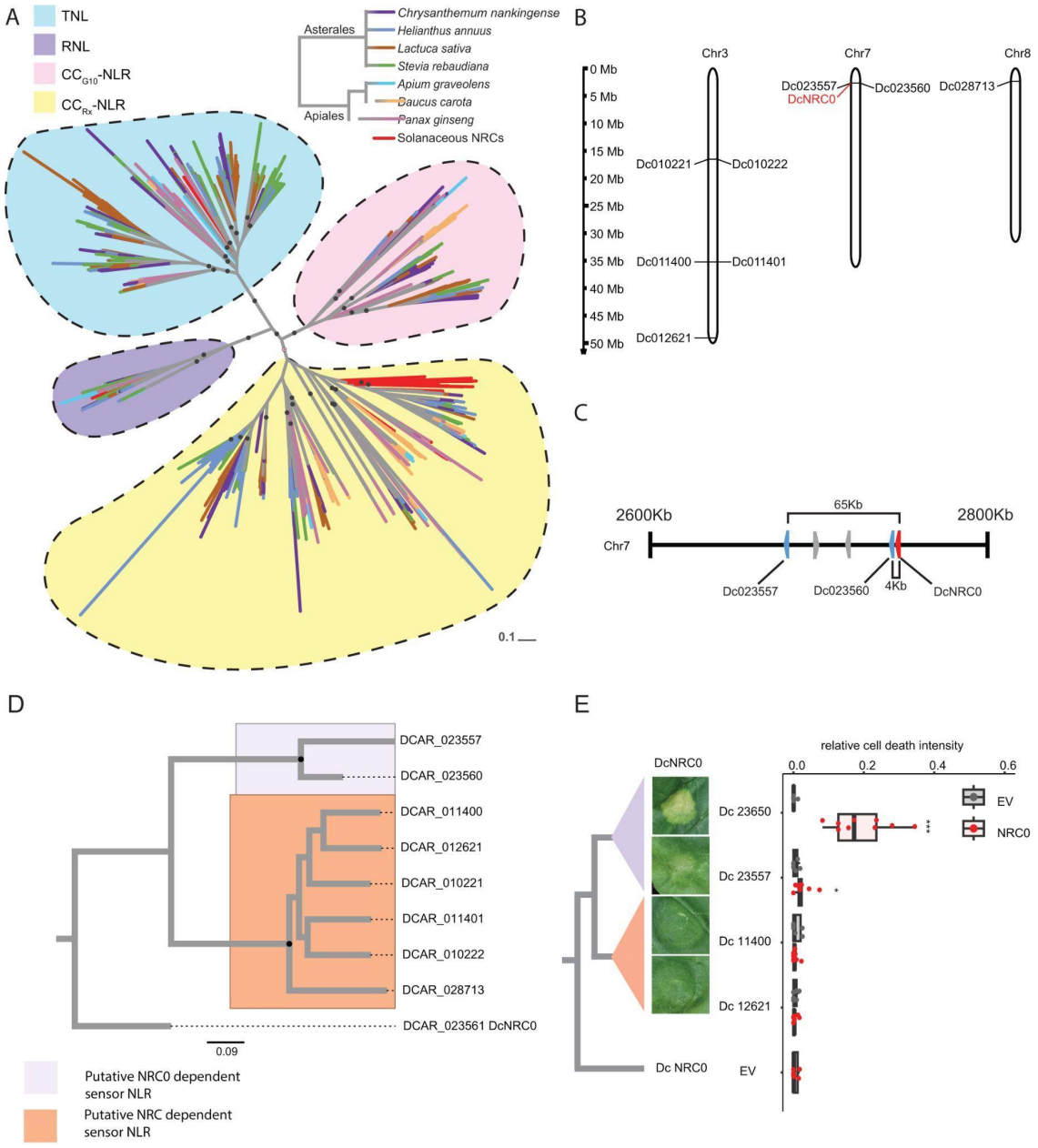

Supplemental Fig. S3. Carrot NRC0-dependent sensor NLRs induce cell death through the linked NRC0. **A)** Phylogenetic analysis of NLRs from 7 species of campanulids. Major nodes with bootstrap values over 70 are indicated with black dots. **B)** The NRC superclade members of carrot (*D. carota*) on chromosome 3, chromosome 7, and chromosome 8. **C)** The NRC0 sensor and helper genes cluster on chromosome 7. **D)** Phylogenetic analysis of the NRC superclade of carrot. Major nodes with bootstrap values over 70 are indicated with black dots. **E)** Cell death assay results of NRC-dependent sensor NLRs co-expressed with the NRCs from carrot in *N. benthamiana* observed at 5 dpi. All sensor NLRs carried the MHD motif (D to V) mutation. The dot plot represents cell death quantification analysed by UVP ChemStudio PLUS. Statistical differences were examined by paired Student's t-test (* = $p < 0.05$, and *** = $p < 0.001$).

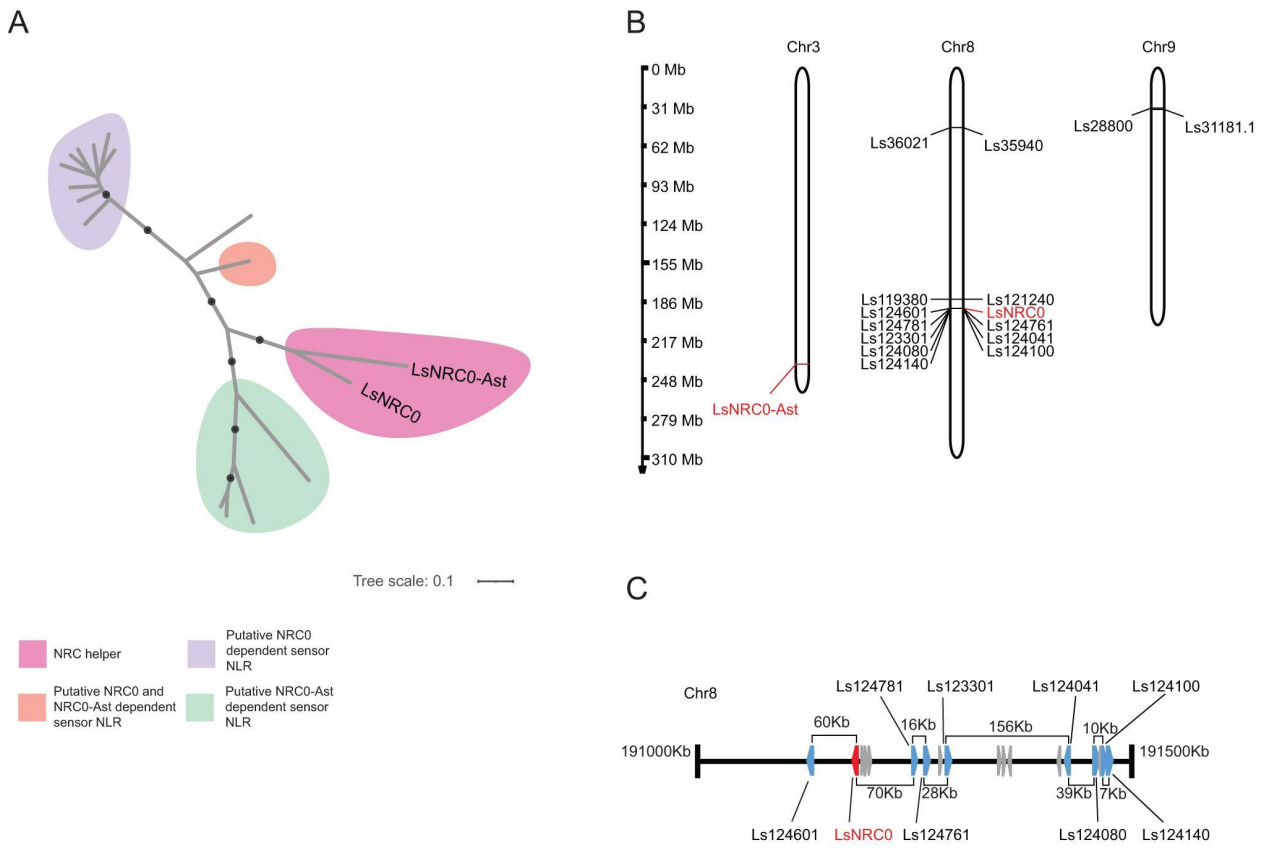

Supplemental Fig. S3. Phylogenetic analysis and gene cluster of the NRC superclade in lettuce. **A)** Phylogenetic analysis of the NRC superclade of *L. sativa*. Major nodes with bootstrap values over 70 are indicated with black dots. **B)** The NRC superclade members of lettuce (*L. sativa*) on chromosome 3, chromosome 8, and chromosome 9. **C)** The NRC0 sensor and helper genes cluster on chromosome 8.

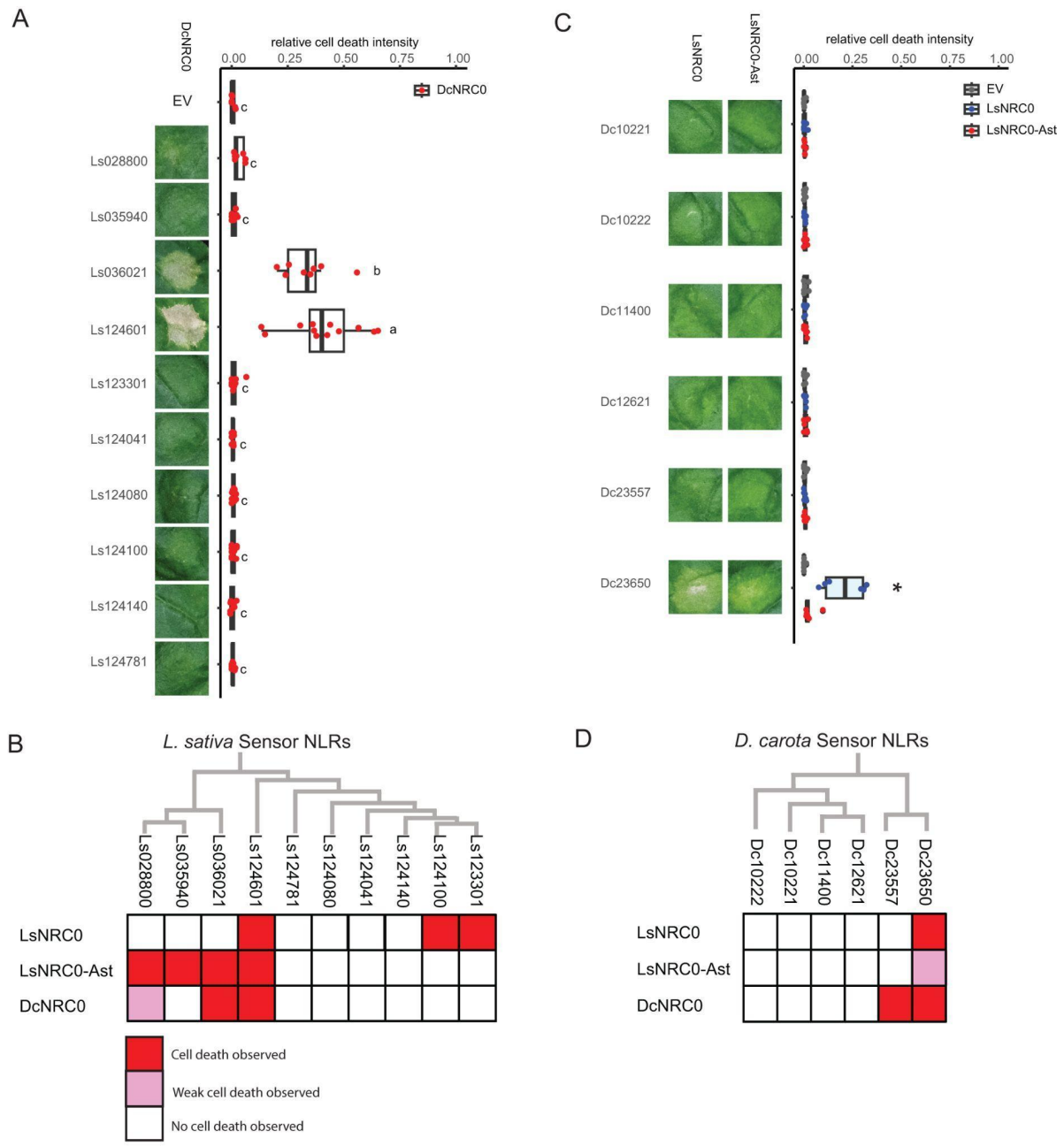

Supplemental Fig. S5. Lettuce LsNRC0 and LsNRC0-Ast are partially interchangeable with carrot DcNRC0. **A)** Cell death assay results of lettuce putative NRC-dependent sensor NLRs co-expressed with carrot NRC0 in *N. benthamiana* observed at 5 dpi. **B)** Matrix of cell death assays for lettuce sensor NLRs co-expressed with lettuce and carrot NRCs, including information obtained in Fig. 3. **C)** Cell death assay results of carrot putative NRC-dependent sensor NLRs co-expressed with lettuce NRCs in *N. benthamiana* observed at 5 dpi. All sensor NLRs carried the MHD motif (D to V) mutation. For (A) and (C), the dot plot represents cell death quantification analysed by UVP ChemStudio PLUS. Statistical differences among the samples were analysed with Tukey's HSD test (* = $p < 0.05$) for each sensor NLR independently. **D)** Matrix of cell death assays for carrot sensor NLRs co-expressed with lettuce and carrot NRC families, including information obtained in Supplemental Fig. S3.

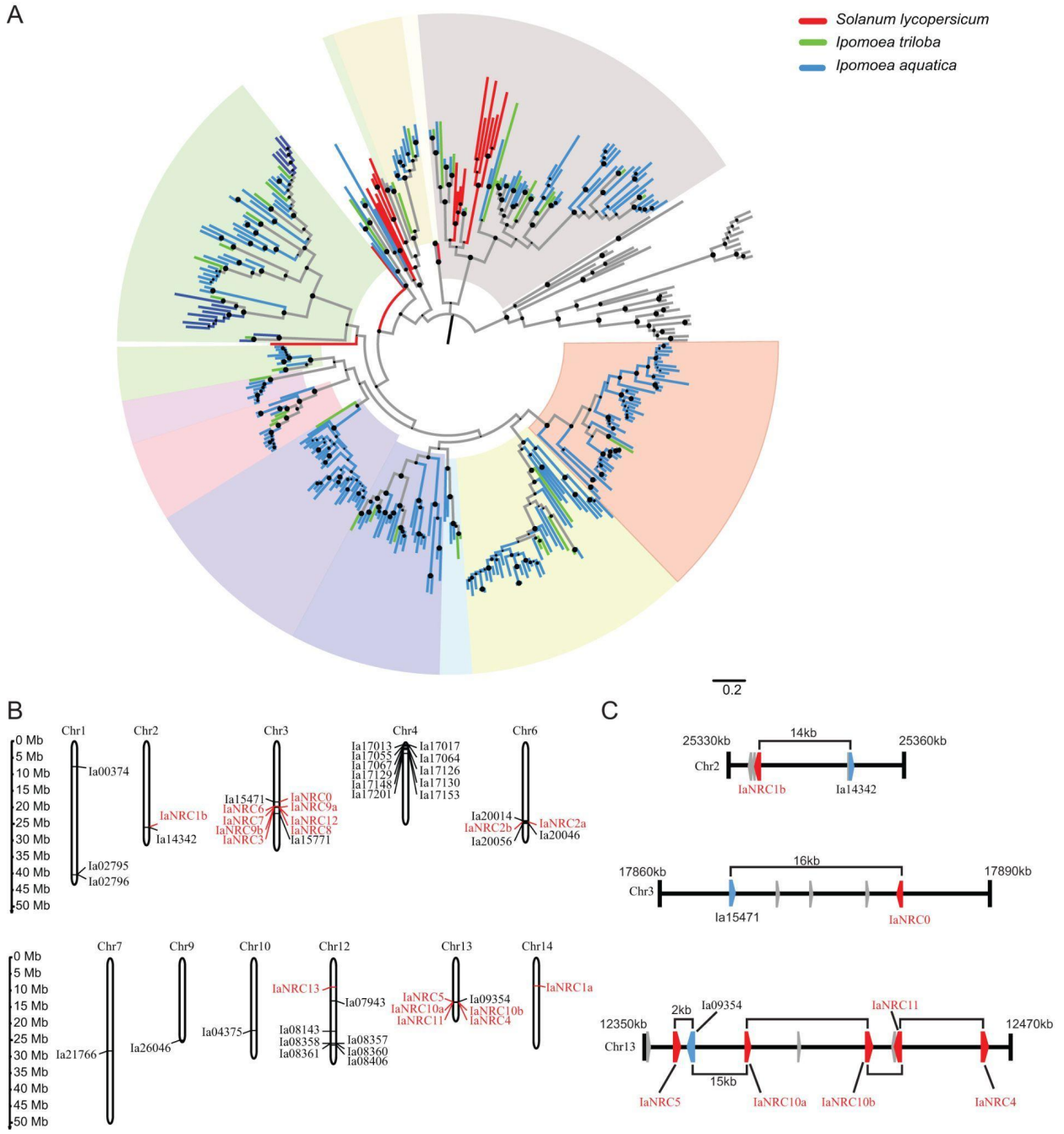

Supplemental Fig. S6. *I. aquatica* has a smaller and simpler NRC network compared to *I. triloba*. **A)** Phylogenetic analysis of the NRC superclade of tomato, *I. triloba*, and *I. aquatica*. Nodes with bootstrap values over 70 are labelled with black dots **B)** The distribution of NRC superclade members of water spinach (*I. aquatica*) on different chromosomes. **C)** The NRC sensor and helper genes cluster on chromosome 2, chromosome 3, and chromosome 13.

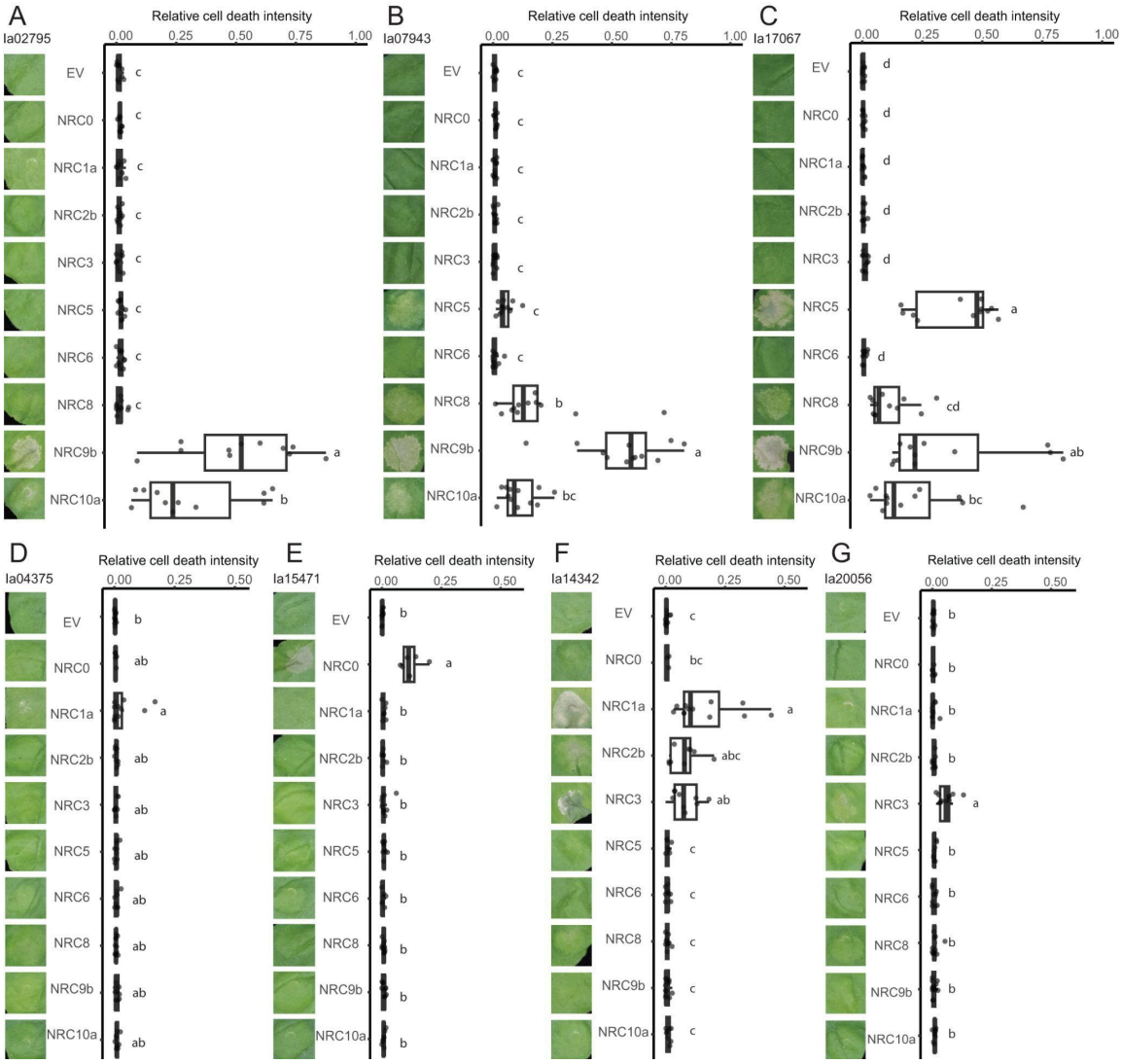

Supplemental Fig. S7. Cell death assay results of *I. aquatica* sensor NLRs co-expressed with Con-IaNRCs in *N. benthamiana* observed at 5 dpi. *I. aquatica* sensor NLRs **A)** Ia02795, **B)** Ia07943, **C)** Ia17067, **D)** Ia04375, **E)** Ia15471, **F)** Ia14342, and **G)** Ia20056 were made into autoactive (D to V mutation in the MHD motif) and then co-expressed with Con-IaNRCs in *N. benthamiana.* The dot plot represents the cell death quantification analysed by UVP. Statistical differences among the samples were analysed with Tukey's HSD test ($p<0.05$).

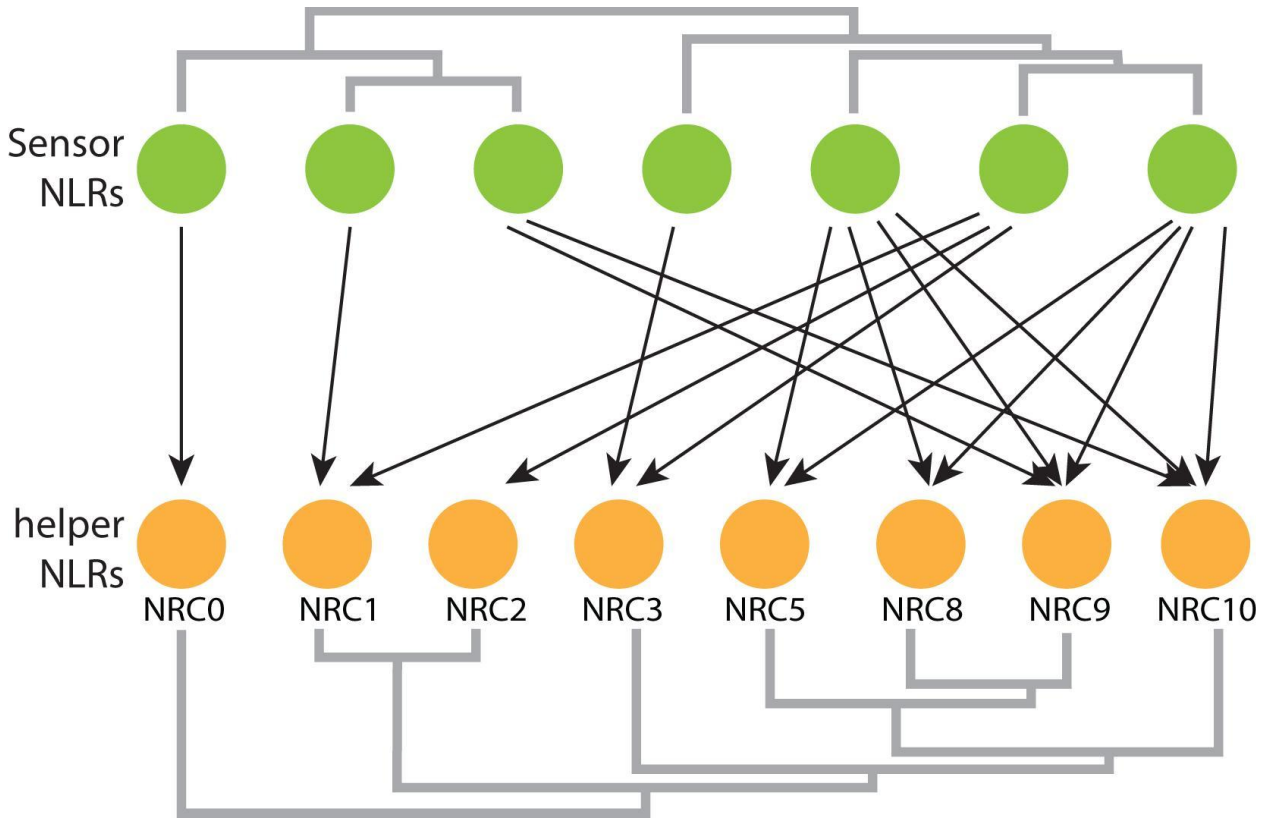

Supplemental Fig. S8. Water spinach possesses a complex NRC network. NRC0 can be specifically triggered by the NRC0-dependent sensor NLR to induce cell death. Certain sensor NLRs signal through Con-IaNRC1 or Con-IaNRC3 to induce cell death. Additionally, some sensor NLRs are capable of signalling through a few other NRC helpers to induce cell death.

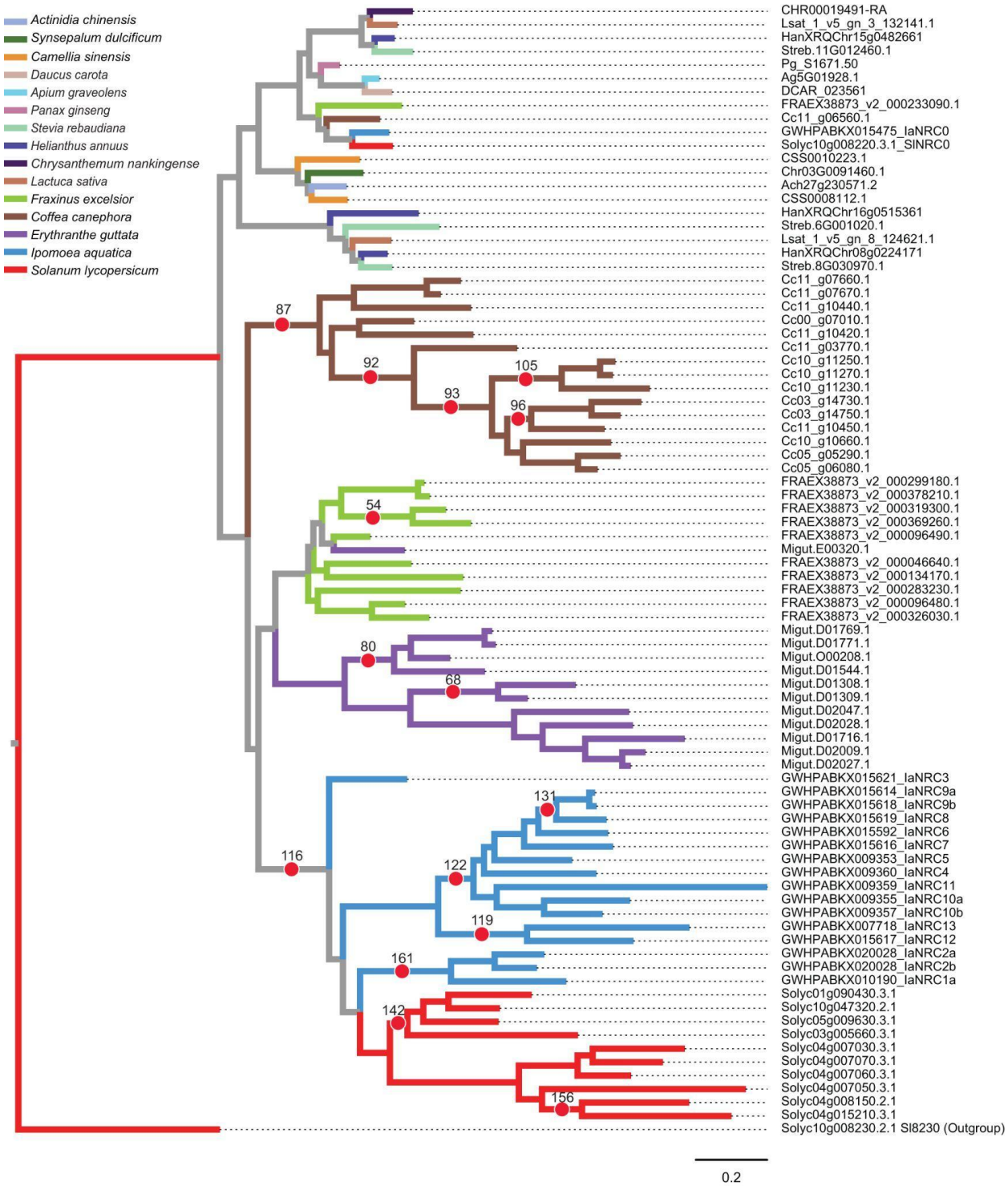

Supplemental Fig. S9. Several nodes in the phylogenetic tree of lamiids family-specific NRC subclades show diversifying selection. Full-length sequences of the NRC family from 15 selected asterids were used to generate the phylogenetic tree. The aBSREL analysis was used to detect internal branches with episodic diversifying selection, based on the Likelihood Ratio Test with a significance threshold set at $p \leq 0.05$. The red dots indicate the 15 nodes showing diversifying selection and the numbers next to the red dots are the corresponding node numbers in the Supplemental Data Set 3.

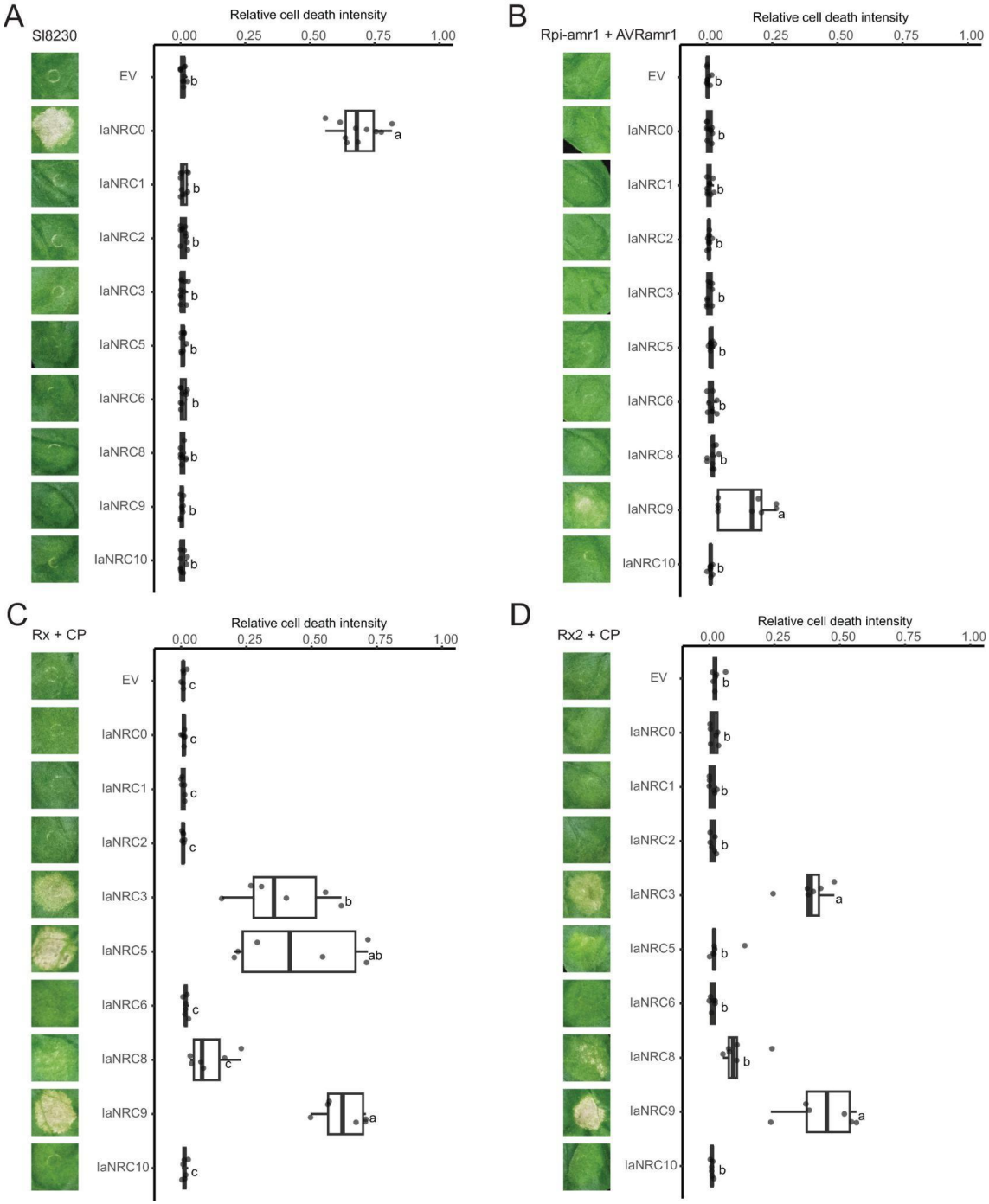

Supplemental Fig. S10. Solanaceous sensor NLR Rx, Rx2 and Rpi-amr1 can signal through some NRCs from *I. aquatica*. Solanaceous sensor NLR **A)** Sl8230 (Solyc10g008230), **B)** Rpi-amr1, **C)** Rx, and **D)** Rx2 were made into autoactive or co-expressed with the corresponding AVRs and Con-IaNRCs in *N. benthamiana* leaves. Cell death phenotypes were recorded at 5 dpi. The dot plot represents the cell death quantification analysed by UVP ChemStudio PLUS. Statistical differences among the samples were analysed with Tukey's HSD test ($p<0.05$).

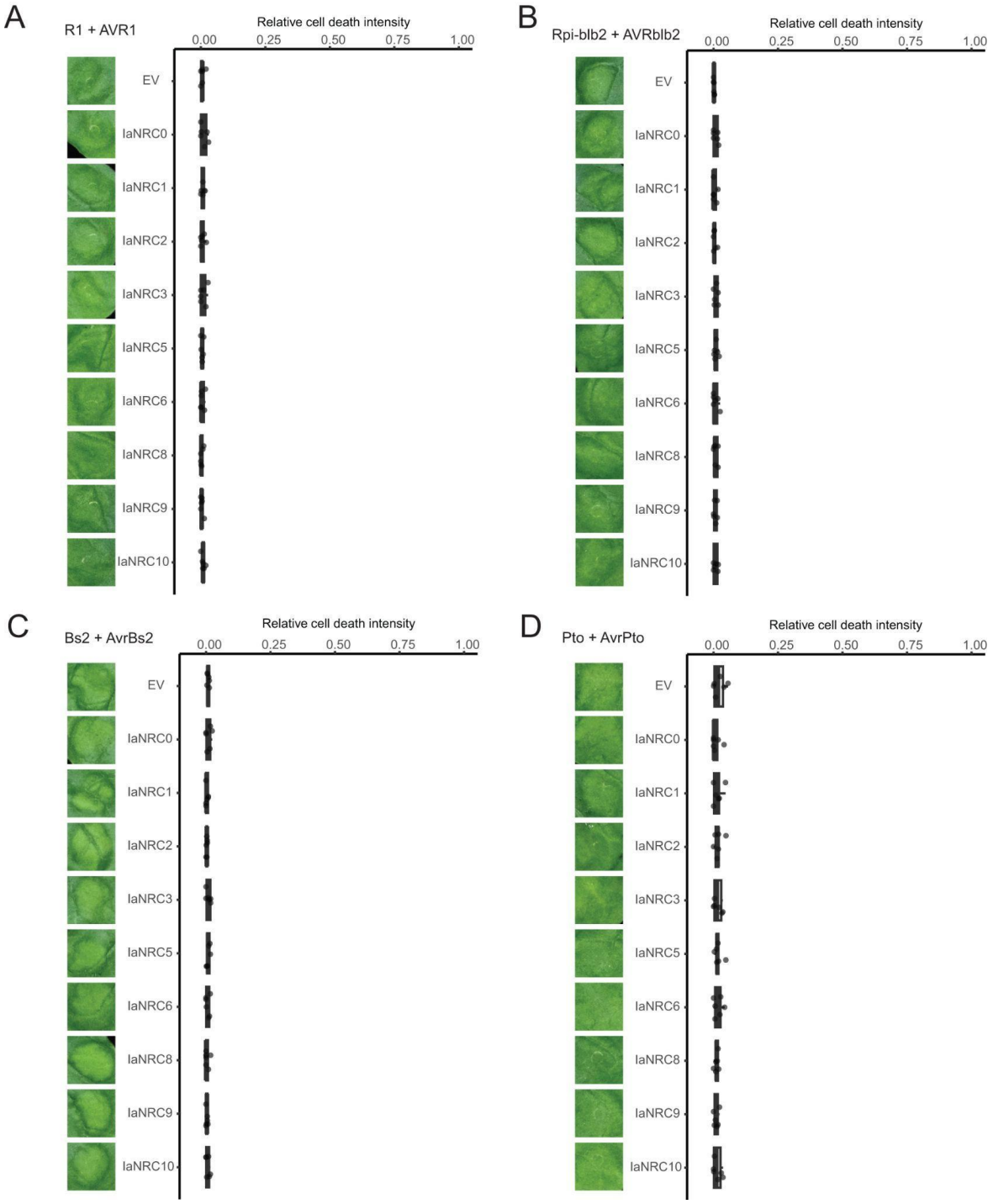

Supplemental Fig. S11. Solanaceous sensor NLRs R1, Rpi-blb2, Bs2, and Prf can not signal through any of the *I. aquatica* NRC tested. Solanaceous sensor NLRs **A)** R1, **B)** Rpi-blb2, **C)** Bs2, and **D)** Prf (Pto) were co-expressed with the corresponding AVRs and Con-IaNRCs in *N. benthamiana* leaves. Cell death phenotypes were recorded at 5 dpi. The dot plot represents the cell death quantification analysed by UVP ChemStudio PLUS. Statistical differences among the samples were analysed with Tukey's HSD test ($p>0.05$).

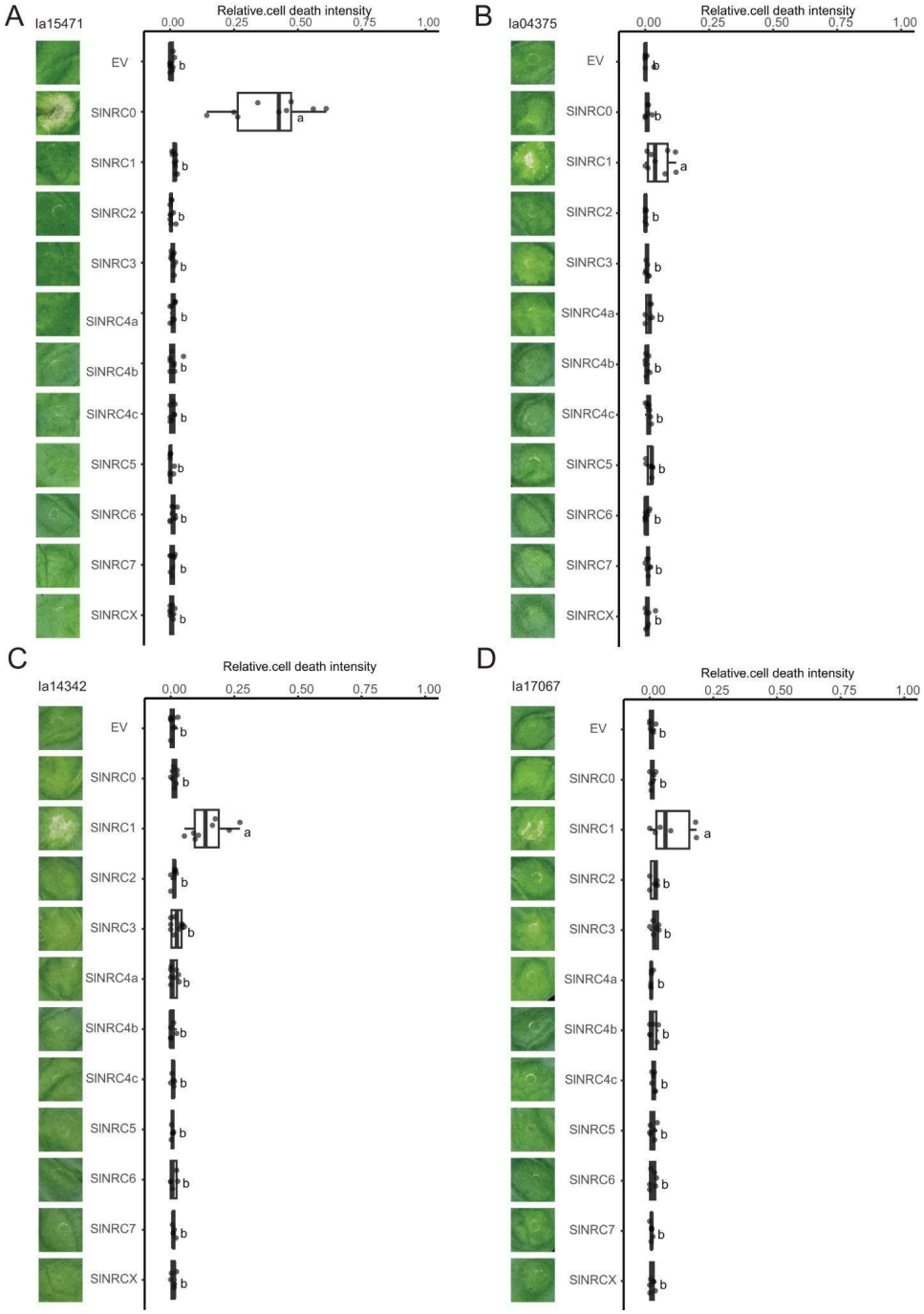

Supplemental Fig. S12. Some *I. aquatica* sensor NLR can signal through NRC1 of tomato. Sensor NLR from *I. aquatica* **A)** Ia15471, **B)** Ia04375, **C)** Ia14342, and **D)** Ia17067 were made into autoactive (D to V mutation in the MHD motif) and then co-expressed with Sol-SlNRCs in *N. benthamiana.* Cell death phenotypes were recorded at 5 dpi. The dot plot represents the cell death quantification analysed by UVP ChemStudio PLUS. Statistical differences among the samples were analysed with Tukey's HSD test ($p<0.05$).

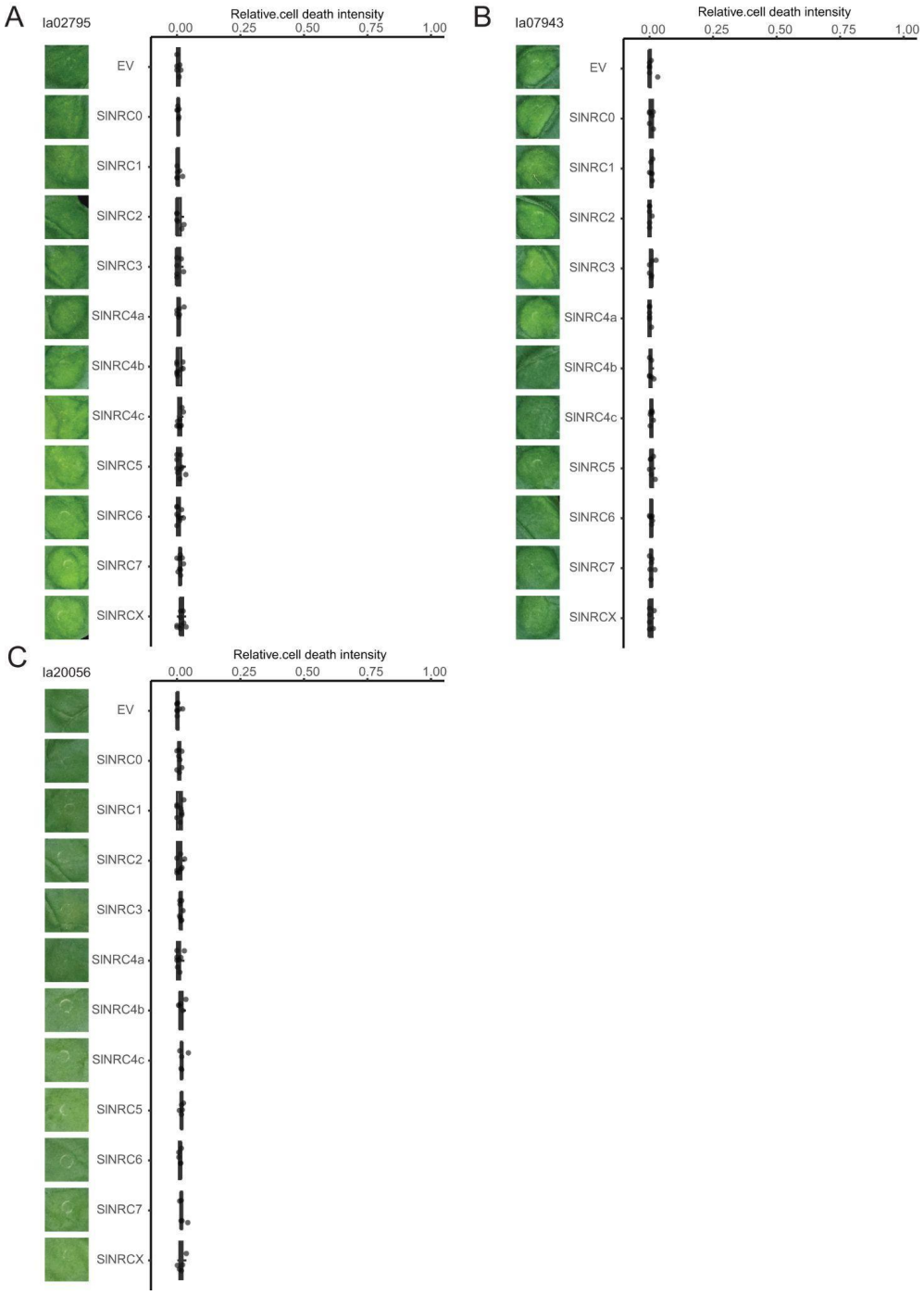

Supplemental Fig. S13. Some *I. aquatica* sensor NLRs can not signal through any of the tomato NRCs tested. Sensor NLR from *I. aquatica* **A)** Ia02795, **B)** Ia07943, and **C)** Ia20056 were made into autoactive (D to V mutation in the MHD motif) and then co-expressed with Sol-SlNRCs in *N. benthamiana.* Cell death phenotypes were recorded at 5 dpi. The dot plot represents the cell death quantification analysed by UVP ChemStudio PLUS. Statistical differences among the samples were analysed with Tukey's HSD test ($p<0.05$).